nature communications

Article

https://doi.org/10.1038/s41467-025-57788-5

Cortico-striatal circuit mechanisms drive the effects of D1 dopamine agonists on memory capacity in mice through cAMP/PKA signalling

Received: 10 November 2023

Accepted: 3 March 2025

Published online: 17 March 2025

Check for updates

Maria De Risi[1,2,8], Diletta Cavezza[1,3,8], Giulia Torromino[1,4], Anita Capalbo[5], Xabier Bujanda Cundin[2], Rosaria Di Martino[5], Filomena Grazia Alvino[1], Attilio Iemolo[6], Luisa Speranza[6], Carla Perrone-Capano[6,7], Marianna Crispino[7], Carmine Cirillo[2], Alberto Luini[5], Francesca Sacco[2], Paolo Grumati[2] & Elvira De Leonibus[1,2]

Working memory capacity (WMC), the number of items remembered in a short-time interval, is regulated by fronto-striatal dopamine (DA) and is reduced in schizophrenia. We investigated how excessive and insufficient D1 dopamine receptor stimulation impairs and expands WMC, focusing on the cAMP/PKA pathway in the fronto-striatal circuit. Low doses of the D1 agonist SKF 38393 enhance WMC by activating the striatum (mice remember more objects), while high doses, paradoxically, impair WMC, activating the same pathway in the medial prefrontal cortex (mPFC) but inhibiting it in the striatum. This impairment, arising from mPFC-driven recruitment of inhibitory striatal parvalbumin interneurons, can be prevented by optogenetic inhibition of the mPFC-striatal pathway. Low doses of SKF 38393 also rescue WMC deficits in a schizophrenia mouse model. These results highlight the need for a systems pharmacology approach that considers complex brain interactions and intracellular signalling pathways, rather than isolated drug-receptor interactions, to develop memory-enhancing treatments.

Working memory (WM), the ability to maintain information for a limited amount of time, is crucial for everyday learning activities and correlates with fluid intelligence in humans. WM not only has a limited duration but also a limited capacity, here defined as working memory capacity (WMC), which is the number of elements that can be processed by the brain in a short-time interval (seconds or minutes), which is about six items in humans and rodents[1,2]. Reduced WMC is a core cognitive symptom of schizophrenia and aging[3,4].

In 1971, Fuster described delayed activity in the prefrontal cortex (PFC)[5]. In 1979, Patricia Goldman-Rakic's landmark paper demonstrated the role of dopamine (DA) within the prefrontal cortex (PFC) as a key modulator of the spatial delayed response task[6]. Then, in 1993, she and her colleagues showed that sustained activity of single prefrontal cortical neurons in alert monkeys served as a neuronal code for WM maintenance[7]. DA has many physiological functions. Depending on the brain regions where it is released (ventral and dorsal

[1]Institute of Biochemistry and Cell Biology (IBBC), National Research Council (CNR), Monterotondo (Rome), Italy. [2]Telethon Institute of Genetics and Medicine (TIGEM), Telethon Foundation, Pozzuoli (Naples), Italy. [3]PhD Program in Behavioral Neuroscience, Sapienza University of Rome, Rome, Italy. [4]Department of Humanistic Studies, University of Naples Federico II, Naples, Italy. [5]Institute of Biochemistry and Cell Biology (IBBC), Naples, Italy. [6]Institute of Genetics and Biophysics (IGB), National Research Council (CNR), Naples, Italy. [7]Department of Biology, University of Naples Federico II, Naples, Italy. [8]These authors contributed equally: Maria De Risi, Diletta Cavezza. e-mail: elvira.deleonibus@cnr.it

striatum-STR, PFC, hippocampus, amygdala), DA modulates reward-coding, locomotor activity, novelty detection, and memory[8,9]. Once released, DA acts on D1-like and D2-like receptors (D1R and D2R) that have opposite effects on the activation of adenylate cyclase, cyclic AMP (cAMP), and protein kinase A (PKA), here referred to as the cAMP/PKA signalling pathway, thereby regulating different behavioural and cognitive processes[10]. Accumulating evidence clearly confirmed that DA has a key role in WM maintenance through its action on D1R. However, previous attempts to use D1R agonists as memory enhancers were limited by the fact that DA produces an 'inverted U-shaped' dose-response curve on cognitive functions[11–15], meaning that both insufficient (as in Parkinson's disease) or excessive (for instance with amphetamine) stimulation of DA receptors result in memory impairment[16–18]. By contrast, moderate doses of DA stimulation (low doses of DA agonists) improve cognition. For example, high doses (1–6 mg/kg) of D1R agonists impair memory[19,20]. In contrast, very low doses (0.00001–0.0001 mg/kg), which mimic the effects of moderate release of DA, improve performance in memory tasks[14,15]. The inverted-U shaped dose-response curve of DA agonists dramatically limits their clinical use and insufficient target engagement[21], despite being safe and well tolerated by human subjects.

Different hypotheses have been proposed to explain the inverted-U dose-response that all focus on their action on the mPFC. Goldman-Rakic and colleagues suggested that low and high concentrations of D1R agonists facilitate or impair WM maintenance by enhancing the activity of prefrontal excitatory or inhibitory neurons, respectively[22]. Another model proposed by Dash and colleagues[23] takes into account the intracellular signalling cascade mediated by D1R stimulation. They suggested that low D1R activation boosts calcium release and calcium-mediated phosphatase activity (i.e., by activating calcineurin), thus improving WM, while higher activation has the opposite effect[23]. More recently, experimental evidence suggested that the dose-dependent effects of D1 agonists on WM depend on their relative "functional selectivity", their preferential action on different intracellular signalling pathways mediated by the same receptor (cAMP or β-arrestin)[24–26].

However, despite decades of research, memory enhancing effects of D1R agonists in the mPFC have been shown for maintenance in temporal terms (number of spikes/sec) rather than in terms of capacity[27], the number of elements remembered during the delay. This raises the question of whether D1R agonists can extend WMC beyond its physiological limit. As WMC correlates with fluid intelligence and its reduction is a core cognitive symptom of schizophrenia[28], WMC expansion has several possible applications.

Interestingly, none of these studies take into account the role of D1R activation in the STR, which is the brain region with the highest D1R density (for review see ref. 29) and thus potentially the first receptors activated by systemic injections of dopaminergic drugs. This pathway is regulated by mPFC inputs and is crucial for goal-directed behaviours and for instrumental learning, but it has been shown to also have a crucial role in WMC. Indeed, in humans, WMC correlates with the total amount of DA in the dorsal STR[30], the activity of which is finely regulated by glutamatergic inputs from the mPFC.

In this study, we explored how D1 agonists regulate WMC by acting on the fronto-striatal circuit. We report that low doses of the D1R selective agonist SKF 38393 (and its analogue SKF 83822) expand incidental WMC in mice and rescue WMC deficits in an animal model of schizophrenia. By contrast, higher doses of SKF 38393 impair performance in normal mice. Using a combination of chemogenetic, pharmacological, optogenetic, and phosphoproteomic approaches, we show that lower and higher doses of SKF 38393 expand and impair WMC by activating the cAMP/PKA pathway in the STR and in the mPFC, respectively. Optogenetic inhibition of the mPFC-STR input precludes the memory impairing effects of the higher dose by preventing the recruitment of striatal parvalbumin (PV) inhibitory interneurons.

Results

D1-like receptor stimulation generates inverted-U dose-response effects on working memory capacity

To test WMC in mice, we used the different/identical-objects-test (DOT/IOT), which is a modified version of the novel object recognition test. In the DOT/IOT, the number of objects that can be remembered varies, resulting in different WMC load, without the need to motivate the animals with a specific reward, similarly to curiosity-driven incidental encoding in humans. In its original version, the DOT measured WMC by increasing the number of different objects to be remembered (i.e., 3, 6 or 8), while the IOT is the control-low WMC test, in which all of the objects presented are identical[2,31,32]. Together, these tests offer important advantages for studying cognitive functions regulated by the dopaminergic system. Based on previous studies[2,32], normal mice were able to recognise up to 6 different objects (6-DOT, which is considered the highest memory load condition), but not 8 (8-DOT) at the 1 min retention interval. Thus, the latter represents a memory overload condition. To test the effects of the pharmacological stimulation of D1R on WMC, mice were injected with increasing doses of SKF 38393 and tested in the 6-DOT. The highest dose (0.1 mg/kg) reduced preference for the novel object, revealing an impairment in a high memory load condition (Fig. 1a, b). The other doses did not affect performance in the 6-DOT. To test whether D1R stimulation expanded WMC, mice were exposed to 8-DOT, the overload condition[2,32], as confirmed by the lack of any preference for the new object in the vehicle group, where almost all mice failed to discriminate the novel object during the test phase (Fig. 1c, d). Interestingly, the low dose of SKF 38393 (0.001 mg/kg) expanded WMC from 6 to 8 objects, as indicated by the increase in the discrimination index observed after treatment in the 8-DOT (Fig. 1c, d). This was not due to non-specific effects on the total distance travelled or the exploratory behaviour (Supplementary Table 1). A similar dose-response effect was observed after systemic treatment with the D1R agonist analogue SKF 83822 (Supplementary Fig. 1a-a'). The different dose-range efficacy of these agonists is consistent with the higher affinity of SKF 38393 for D1R compared to SKF 83822[33].

Overall, these data show that D1R agonists expand WMC at low doses (hereafter referred to as improving dose) and impair it at higher doses (hereafter referred to as impairing dose). To confirm that these effects were D1R-dependent, we conducted a pharmacological experiment in which we treated mice with a high dose of SKF 38393 combined with the selective D1 antagonist SCH-23390, at a dose previously shown to be ineffective on WMC when administered alone[31]. As expected, combining the ineffective dose of SCH-23390 (0.001 mg/kg) with 0.1 mg/kg SKF38393 rescued the SKF-induced impairment of WMC, suggesting that this effect was D1R-dependent (Fig. 1e, f).

Improving and impairing doses of SKF 38393 differentially activate the striatum and the medial prefrontal cortex

To identify the mechanism mediating these improving- and impairing-WMC effects at the molecular and circuit level, we first performed c-Fos immunostaining, focusing on the fronto-striatal circuit. c-Fos is an immediate early gene which is used as a marker of neuronal activity. c-Fos-positive (c-Fos$^+$) cells increased in the mPFC after treatment with the impairing dose, both in the cingulate cortex (Cg) and in the prelimbic/infralimbic cortex (PrL/IL) (Fig. 2a-a'), but not with the improving one (Fig. 2a-a'). In contrast, the improving dose led to a significant increase in the number of c-Fos$^+$ cells in the STR (Fig. 2b-b'), which was greater in the dorso-medial striatum (DMS) compared to the dorso-lateral striatum (DLS) (Fig. 2b-b'). To rule out the possibility that higher doses of SKF recruited fewer D1$^+$ striatal neurons, the percentage of c-Fos$^+$/D1R$^+$ cells in the striatum was evaluted[34,35]. The proportion of c-Fos$^+$/D1R$^+$ cells was similar

https://doi.org/10.1038/s41467-025-57788-5

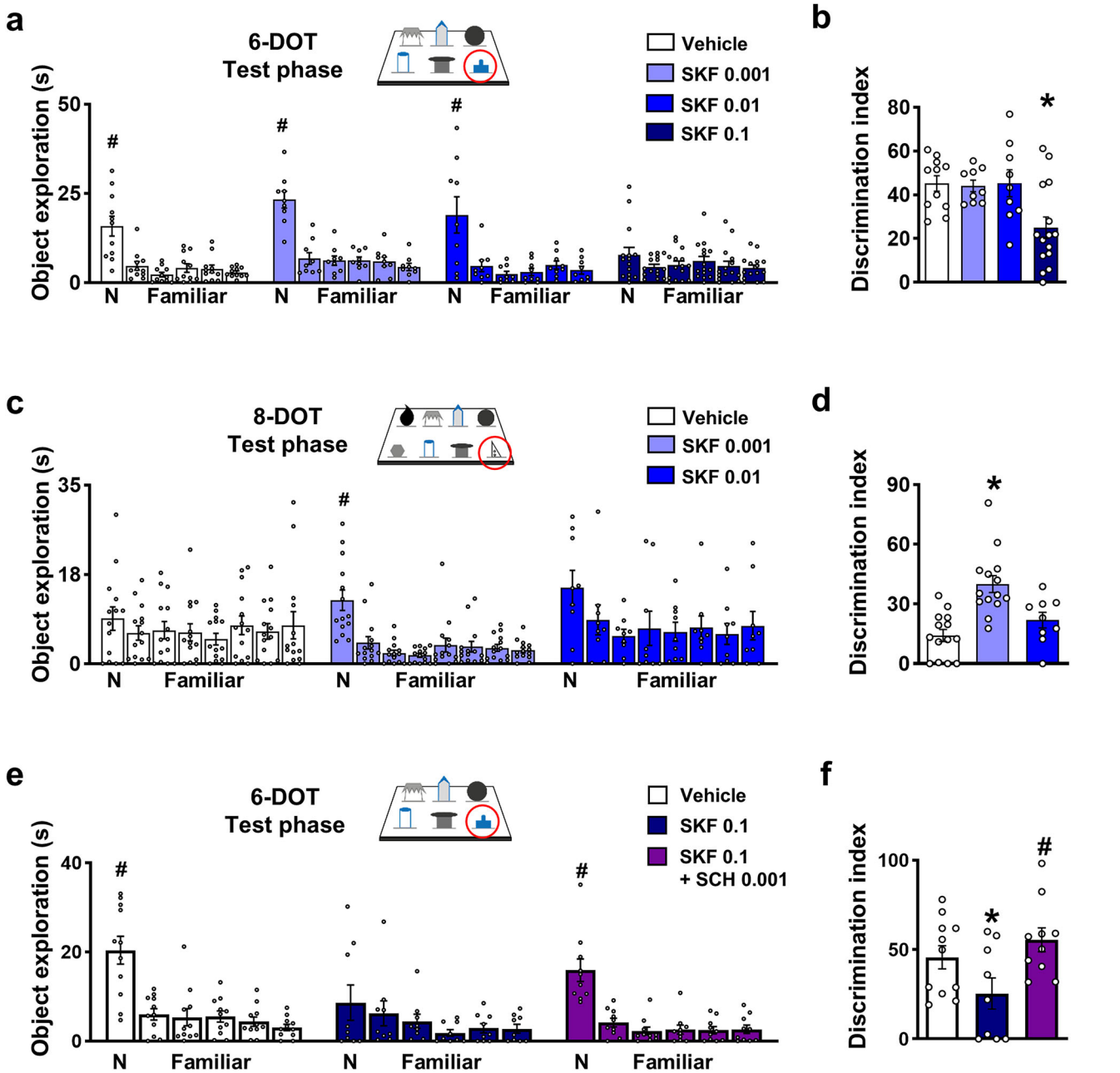

Fig. 1 | SKF 38393 exerts inverted-U dose-response effects on memory capacity. **a** Effects of increasing doses of SKF 38393 (0.001, 0.01 and 0.1 mg/kg) on single object exploration (Repeated measures ANOVA: Treatment: $F_{3,40} = 2.68$; $p = 0.0593$; Object $F_{5,200} = 44.28$; $p < 0.0001$; Treatment x Object $F_{15,200} = 3.9$; $p < 0.0001$, Dunnett's post hoc) and **(b)** on the discrimination index during the 6 different objects test (6-DOT) (One-way ANOVA: Treatment: $F_{3,40} = 5.42$; $p = 0.0032$, Tukey's post hoc). **c** Effects of increasing doses of SKF 38393 (0.001 and 0.01 mg/kg) on single object exploration (Repeated measures ANOVA: Treatment: $F_{2,34} = 2.39$; $p = 0.1061$; Object $F_{7,238} = 8.9$; $p < 0.0001$; Treatment x Object $F_{14,238} = 1.38$; $p = 0.1628$, Dunnett's post hoc) and **(d)** on discrimination index during the 8 different objects test (8-DOT) (One-way ANOVA: Treatment: $F_{2,34} = 13.5$; $p < 0.0001$, Tukey's post hoc). **e** Effects of SKF 38393 0.1 mg/kg combined with SCH-23390 (0.001 mg/kg) on single object exploration (Repeated measures ANOVA: Treatment: $F_{2,27} = 1.94$; $p = 0.1631$; Object $F_{5,135} = 23.1$; $p < 0.0001$; Treatment x Object $F_{10,135} = 2.3$; $p = 0.0157$, Dunnett's post hoc) and **(f)** on the discrimination index during the 6-DOT (One-way ANOVA: Treatment: $F_{2,27} = 5.80$; $p = 0.0080$, Tukey's post hoc). In the upper panel was reported a scheme of the test phase of the 6 or 8-DOT. The red circle indicates the novel object. The histogram reported the exploration of the novel object (N) *versus* the familiar ones. Data are mean values ± SEM. *$p < 0.05$ SKF vs vehicle; #$p < 0.05$ novel object (N) vs familiar. Source data are provided as a Source Data file.

across conditions after both SKF 38393 doses: 83% in the DMS improving dose, 89% in the DMS impairing dose; 88% in the DLS improving dose, 72% in the DLS impairing dose (Supplementary Fig. 2a-a'). This makes it highly unlikely that there was a dose-dependent shift in D1-D2 pathway activation.

To test whether increased c-Fos activation was preceded by activation of the cAMP/PKA pathway, which is a downstream target of D1R activity, we performed Western blot analysis using a phospho-PKA substrate antibody[36,37]. As with c-Fos staining, we observed increased phosphorylation of PKA substrates in the mPFC at the impairing dose (Fig. 3a), while the improving dose increased phosphorylation of PKA substrates in the STR (Fig. 3b). The increase in phosphorylation did not correlate with changes in the expression of the PKA catalytic subunit (C-alpha) (Supplementary Fig. 3a, b).

https://doi.org/10.1038/s41467-025-57788-5

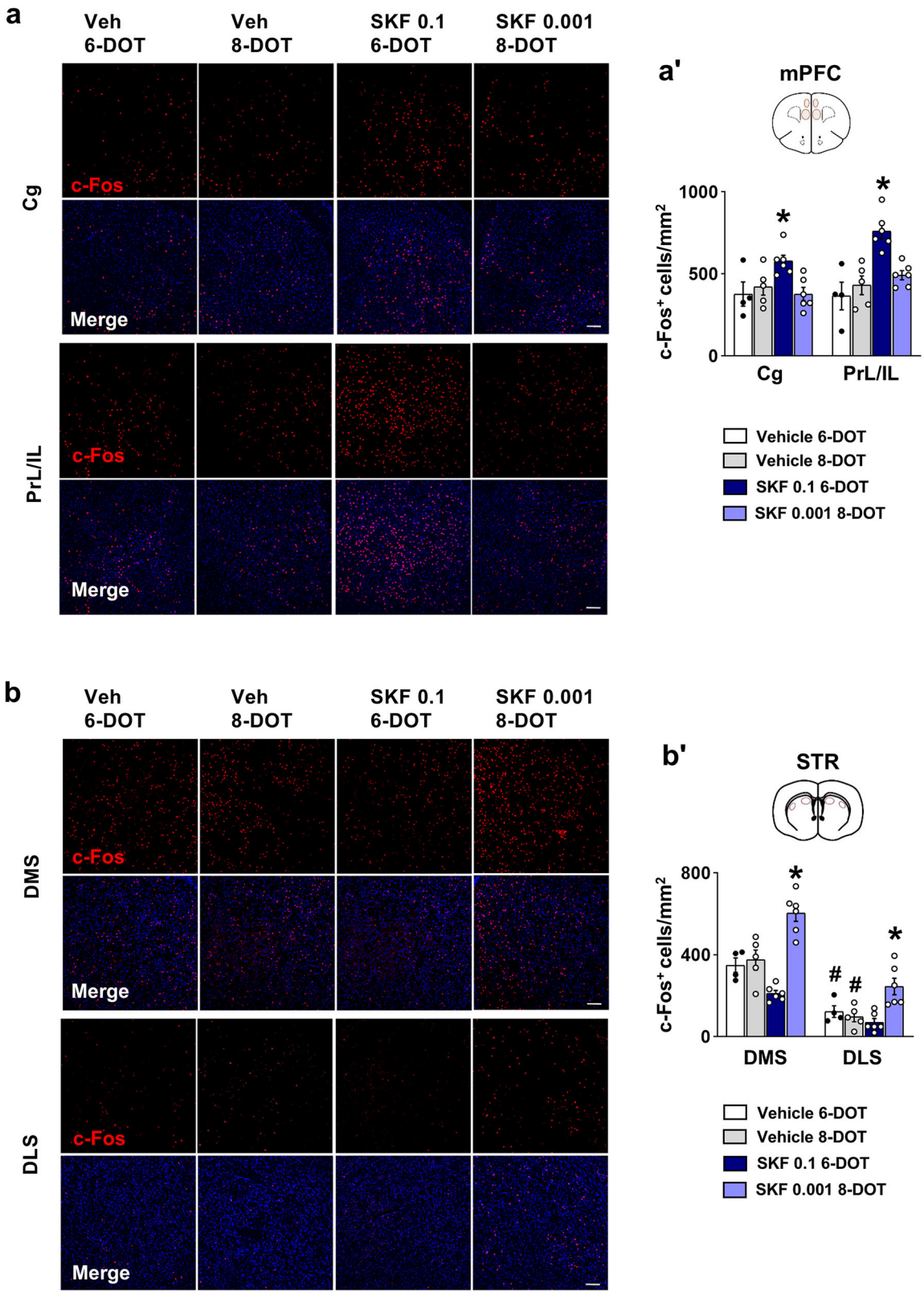

Interestingly, there was a positive correlation between the discrimination index and the level of phosphorylation of substrates in the STR, indicating that higher PKA activation was associated with better performance in the behavioural test (Supplementary Fig. 3c). The activity of PKA in the hippocampus, as expected[38], did not change after SKF 38393 treatment (Supplementary Fig. 3d, e). These results suggest a dose-dependent pattern of PKA activation in the fronto-striatal circuit. In particular, the improving dose of SKF 38393 stimulated PKA activation in the STR, while the higher and impairing dose stimulated its activation in mPFC, and simultaneously prevented it in the STR. As previously shown, the pattern of PKA modulation was paralleled by c-Fos activation in the two brain regions, suggesting a dose-dependent modulation of an input projecting from mPFC to STR that regulates its effect on MC.

https://doi.org/10.1038/s41467-025-57788-5

Fig. 2 | Improving and impairing doses of SKF 38393 increase c-Fos⁺ cells in the striatum and the medial prefrontal cortex, respectively. a, **b** Representative images of c-Fos-immunofluorescence staining in the **(a)** cingulate cortex (Cg) and prelimbic/infralimbic cortex (PrL/IL) and **(b)** the dorso-medial and dorso-lateral striatum (DMS and DLS) of animals tested in the 6-DOT and the 8-DOT injected with vehicle (Veh), the improving dose (0.001 mg/kg), or the impairing dose (0.1 mg/kg) of SKF 38393. **a'**, **b'** Quantification of the number of c-Fos⁺ cells/mm² after SKF 38393 treatment in Cg and PrL/IL of medial prefrontal cortex (mPFC) (Repeated measures ANOVA: Treatment: $F_{3,17} = 9.1$; $p = 0.0008$; Subregion: $F_{1,17} = 11.65$; $p = 0.0033$; Treatment x Subregion; $F_{3,17} = 4.5$; $p = 0.0165$, Tukey's post hoc) and in the DMS and DLS of striatum (STR) (Repeated measures ANOVA: Treatment: $F_{3,17} = 17.9$; $p < 0.0001$; Subregion: $F_{1,17} = 188.4$; $p < 0.0001$; Treatment x Subregion; $F_{3,17} = 10.6$; $p = 0.0003$, Tukey's post hoc). Brain regions were highlighted with red circles in the upper panel. Data are mean values ± SEM. *$p < 0.05$ SKF vs vehicle; #$p < 0.05$ DLS vs DMS. Scale bars: 50 μm. Source data are provided in the Source Data file.

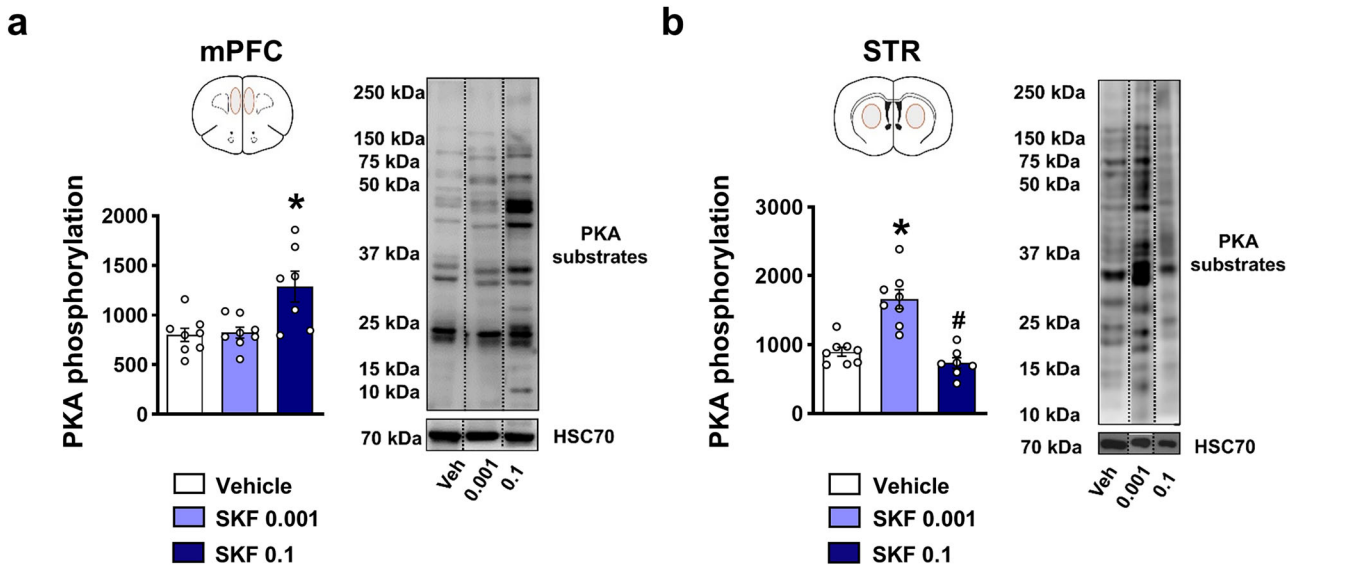

Fig. 3 | Improving and impairing doses of SKF 38393 activate PKA/cAMP signalling in the striatum and the medial prefrontal cortex, respectively. a, **b** Histograms on the left show the quantification of PKA-phosphorylated substrates, which was expressed as the sum of percentage difference of each band relative to the control. Representative immunoblots of protein extracts from the medial prefrontal cortex (mPFC) and the whole striatum (STR) (red circles in the pictures) probed with a phospho-PKA substrate antibody are reported on the right. Hsc70 was used as a loading control. We observed increased phosphorylation of PKA substrates in the mPFC at the impairing dose (One-way ANOVA: Treatment: $F_{2,20} = 7.69$; $p < 0.0033$, Tukey's post hoc), while the improving dose increased phosphorylation of PKA substrates in the STR (One-way ANOVA: Treatment: $F_{2,20} = 24.86$; $p < 0.0001$, Tukey's post hoc). Data are mean values ± SEM. *$p < 0.05$ SKF vs vehicle; #$p < 0.05$ SKF 0.001 vs SKF 0.1. Source data are provided in the Source Data file.

Dose-dependent SKF 38393 effects on striatal phosphoproteomics

The observed correlation between striatal activation and expanded WMC is in line studies in humans showing that WMC correlates with striatal DA release capacity[30]. Since SKF 38393 exerted its action by activating the cAMP/PKA cascade, and the improving and impairing effects of SKF 38393 on WMC seemed to be mediated by hyperactivation and hypoactivation of the STR, respectively, we sought to confirm these data using phosphoproteomics. A heatmap of the 50 most variable phosphorylation sites (phosphosites) suggested that the improving SKF 38393 dose had a unique phosphorylation pattern that was very different from both vehicle- and impairing dose-treated animals (Fig. 4a). Indeed, among the identified phosphosites, 672 were found to be differentially regulated between the improving dose and vehicle treatment, while only 43 changed between the impairing dose and vehicle treatment (Fig. 4b).

As expected, the improving dose of SKF 38393 changed the phosphorylation of many STR proteins that are downstream effectors of cAMP signalling, including the catalytic subunit of PKA itself, and canonical PKA targets such as the glutamate ionotropic receptor NMDA type subunit 2A and subunit 2B (GluN2A and GluN2B), and the dopamine and cAMP-regulated phosphoprotein of 32 kilodaltons (DARPP-32) (Fig. 4c). Moreover, as already reported[39,40], the stimulation of D1R leads to the activation of cAMP-independent signalling pathways, such as Phospholipase C (PLC)/Protein kinase C (PKC), the calmodulin-dependent protein kinase cascade (CaMK), and the extracellular-regulated kinases ERK1/2, that are mediated by direct PKA phosphorylation of RasGRP2 (Fig. 4c). The most abundant phosphosites are reported in Supplementary Fig. 4. These data were supported by a gene ontology (GO) analysis, which showed an up-regulation of the cAMP signalling pathway and increased D1R binding (Fig. 4d). Moreover, we found biological processes linked to synaptic transmission and synaptic signalling to be up-regulated (Fig. 4d). Finally, a cellular component enrichment analysis suggested greater involvement of components like neuron projection, synapses, and axons (Fig. 4d).

The impairing dose led to few changes in upregulated and downregulated phosphosites, which was in line with the hypoactivity detected by Western blotting and c-Fos immunostaining. However, a strong activation of phosphodiesterase (PDE) activity (PDE1, PDE4 and PDE7) was observed, which is known to constrain cAMP increase (Fig. 4e, f), providing a molecular mechanism for such a disengagement.

Together, these results suggest that SKF 38393 induces a dose-dependent pattern of activation of the cAMP/PKA pathway in the STR, which is activated by the low improving dose but not by the high impairing dose.

Pharmacological and chemogenetic inhibition of D1R downstream signalling in the STR counteracts the increase in memory capacity mediated by SKF 38393

To test whether the changes in the cAMP/PKA pathway identified here account for the expanded WMC mediated by the improving dose of

https://doi.org/10.1038/s41467-025-57788-5

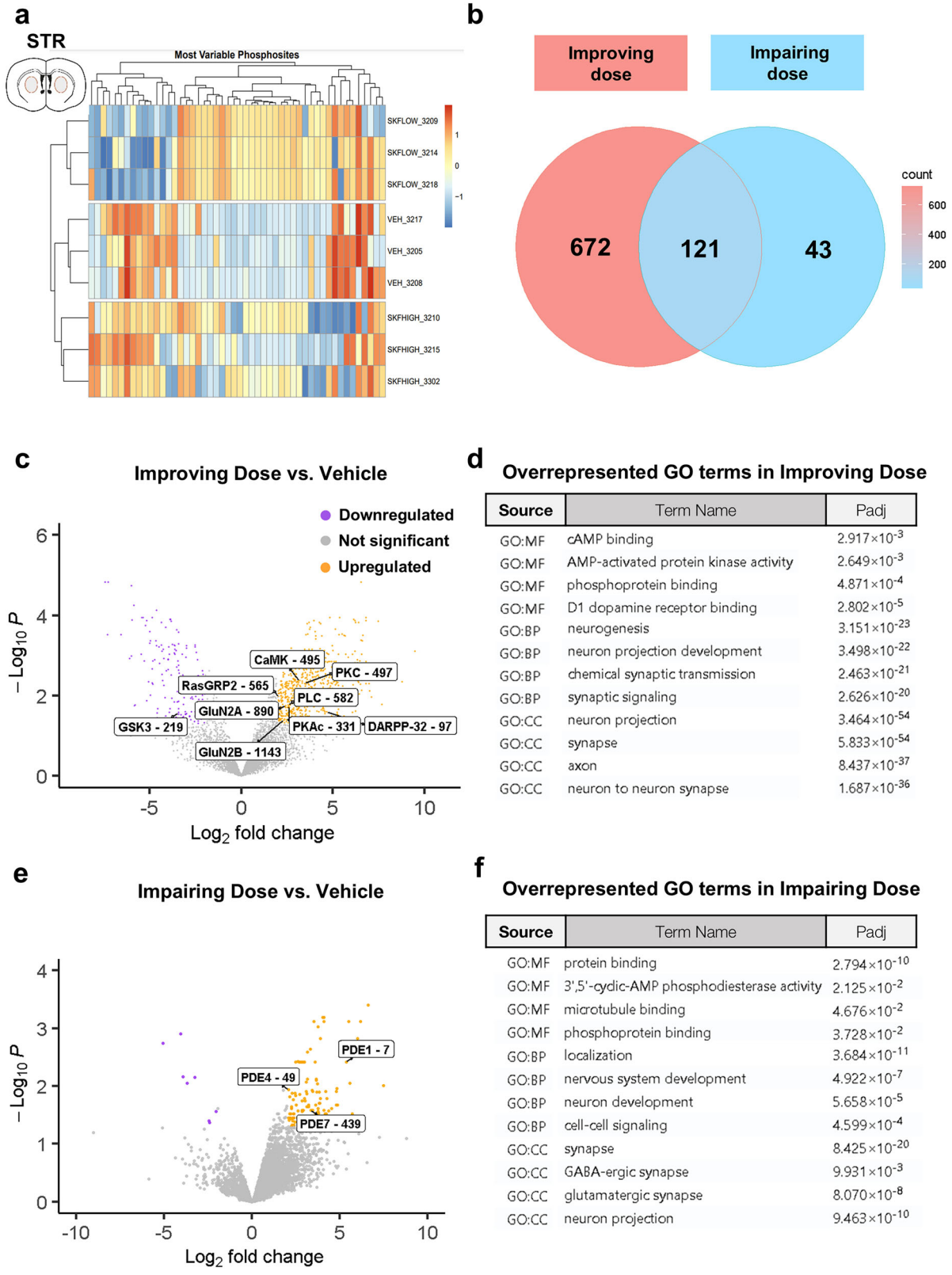

Source	Term Name	Padj
GO:MF	cAMP binding	2.917×10^{-3}
GO:MF	AMP-activated protein kinase activity	2.649×10^{-3}
GO:MF	phosphoprotein binding	4.871×10^{-4}
GO:MF	D1 dopamine receptor binding	2.802×10^{-5}
GO:BP	neurogenesis	3.151×10^{-23}
GO:BP	neuron projection development	3.498×10^{-22}
GO:BP	chemical synaptic transmission	2.463×10^{-21}
GO:BP	synaptic signaling	2.626×10^{-20}
GO:CC	neuron projection	3.464×10^{-54}
GO:CC	synapse	5.833×10^{-54}
GO:CC	axon	8.437×10^{-37}
GO:CC	neuron to neuron synapse	1.687×10^{-36}

Source	Term Name	Padj
GO:MF	protein binding	2.794×10^{-10}
GO:MF	3',5'-cydic-AMP phosphodiesterase activity	2.125×10^{-2}
GO:MF	microtubule binding	4.676×10^{-2}
GO:MF	phosphoprotein binding	3.728×10^{-2}
GO:BP	localization	3.684×10^{-11}
GO:BP	nervous system development	4.922×10^{-7}
GO:BP	neuron development	5.658×10^{-5}
GO:BP	cell-cell signaling	4.599×10^{-4}
GO:CC	synapse	8.425×10^{-20}
GO:CC	GABA-ergic synapse	9.931×10^{-3}
GO:CC	glutamatergic synapse	8.070×10^{-8}
GO:CC	neuron projection	9.463×10^{-10}

SKF 38393 (0.001 mg/kg), we analysed the effects of cAMP agonists and antagonists in the STR. All brain-site manipulations were done in DMS, consistently with the activation pattern. The cAMP antagonist (RP)-cAMPS (here referred to as Rpc)[41] alone impaired performance in the 6-DOT in a dose-dependent manner (Supplementary Fig. 5), without having any significant effect on locomotion or on exploration activity during the study phase (Supplementary Table 2). To test whether the increased MC (performance in the 8-DOT) was mediated by cAMP/PKA activation within the STR, another cohort of animals was systemically injected with the improving dose of SKF 38393 and concurrently injected intra-STR with Rpc, at a dose that, when administered alone, did not affect performance in the 6-DOT, with the aim of blocking PKA substrate phosphorylation and MC improvement (Fig. 5a). The results showed that the pro-cognitive effects of SKF

Fig. 4 | Phosphoproteomic analysis in the striatum revealed a unique pattern of phosphorylation after a low dose of SKF 38393. a Heat map of the 50 most variable phosphosites in mice striatum (STR) treated with vehicle (VEH), an improving dose (SKF-LOW), or an impairing dose (SKF-HIGH) of SKF 38393. The phosphosites with increased intensities are marked in red and the phosphosites with lower intensities are marked in blue. **b** Venn Diagram of differentially expressed phosphosites in mice treated either with vehicle, an improving dose, or an impairing dose. **c** Volcano plot of the phosphosites belonging to the low improving dose relative to vehicle based on the average ratio of three technical replicates and p-value (− log10 p-value). Grey points represent unchanged proteins, and orange and purple represent the upregulated and downregulated proteins, respectively. The indicated proteins are discussed in the text. **d** GO terms over-represented in the low improving versus vehicle comparison. GO:MF refers to Gene ontology Molecular Function, GO:BP refers to the Gene Ontology Biological processes and GO:CC refers to the Gene Ontology Cellular Components. **e** Volcano plot of the phosphosites belonging to the high impairing dose versus vehicle comparison according to the average ratio of three technical replicates and p-value (− log10 p-value). Grey points represent unchanged proteins, and orange and purple represent the upregulated and downregulated proteins respectively. The indicated proteins are discussed in the text. **f** GO terms overrepresented in the high impairing dose versus vehicle comparison. GO:MF refers to Gene ontology Molecular Function, GO:BP refers to the Gene Ontology Biological processes and GO:CC refers to the Gene Ontology Cellular Components. Differential abundance of phosphosites analysis was performed using the one way ANOVA test with a threshold of FDR < 0.05. Source data are provided in the Source Data file.

38393 in the 8-DOT were reversed by the intra-striatal injection of Rpc (Fig. 5a′), while no significant effect was observed on locomotor activity or on object exploration during the study phase (Supplementary Table 2). The behavioural effects were accompanied by reduced phosphorylation of PKA substrates (Fig. 5a″).

To further investigate the pathway underlying the increase in WMC induced by SKF 38393, we used a chemogenetic approach involving viral-mediated gene transfer to express engineered Designer Receptors Exclusively Activated by Designer Drugs (DREADDs), which leads to activation or inhibition of the drug target in a specific brain region[42] (Fig. 5b). First, we injected an inhibitory DREADD (AAV2/5-CaMKIIa-HA-rM4D(Gi)-IRES-mCitrine (hereon referred to as AAV-Gi) into the STR to mimic the effects of Rpc. Infection with the AAV-Gi was verified by immunofluorescence analysis of the haemagglutinin tag (HA) contained within the vector (Fig. 5b). Clozapine N-oxide (CNO), which binds DREADDs, reversed the WMC improvement mediated by low dose SKF 38393 (Fig. 5b′) without affecting mice exploration during the study phase or their locomotor activity (Supplementary Table 2). The control group, which received CNO alone, did not discriminate the novel object, as expected (Fig. 5b′). In the STR of CNO plus SKF-injected mice, there was a decrease in PKA activity compared to those injected with the improving dose of SKF alone (Fig. 5b″).

Thus, pharmacological and chemogenetic inhibition of D1R downstream signalling in the STR prevented the WMC increase mediated by SKF 38393.

cAMP/PKA activation in the striatum is sufficient to expand memory capacity

We next asked whether cAMP/PKA activation in the STR is sufficient to expand WMC above its normal limit (from 6 to 8 objects). To test this hypothesis, we first injected the cAMP agonist, (Sp)-cAMPS (hereafter referred as Spc) into the STR and tested mice in the 8-DOT (Fig. 5c). Results showed that both Spc and SKF 38393 (0.001 mg/kg) allowed animals to recognise the new object among the familiars, thus expanding MC from 6 to 8 objects (Fig. 5c′). No effect was observed on total exploration or locomotion during the habituation phase (Supplementary Table 3). Intra-striatal injection of Spc also led to comparable levels of phosphorylation of PKA substrates observed after systemic injection of the improving dose of SKF 38393 (Fig. 5c″). To test whether striatal activation increased MC, we overexpressed the AAV2/5-CaMKIIa-HA-rM3D (Gs)-IRES-mCitrine (activatory DREADD, here referred as AAV-Gs) within the STR (Fig. 5d). Again, we verified the infection with the AAV-Gs using immunofluorescence analysis for the HA tag (Fig. 5d). CNO-injected animals successfully performed the 8-DOT (Fig. 5d′) and activated the cAMP/PKA pathway compared to the vehicle group (Fig. 5d″), although CNO-injected animals showed a decrease in total exploration during the study phase (Supplementary Table 3). These data indicate that activation of the cAMP/PKA intracellular pathway in the STR is sufficient to increase WMC, also independently of SKF 38393 treatment.

SKF 38393 impairs WMC by simultaneously activating the cAMP/PKA pathway in the mPFC and reducing it in the striatum via fronto-striatal recruitment of parvalbumin- inhibitory interneurons

The highest dose of SKF 38393 (0.1 mg/kg) impaired performance in the 6-DOT (Fig. 1) and simultaneously favoured the activation of the cAMP/PKA pathway in the mPFC but not in the STR (Fig. 3) This suggested that the two events were either independently mediated by the action of the drug in the two brain regions or that hyperactivation of cAMP/PKA in the mPFC might prevent striatal engagement and impair performance in the 6-DOT. To test this hypothesis, we first used a pharmacological approach. We systemically administered the impairing dose of SKF 38393 (0.1 mg/kg) – as previously done – and the cAMP inhibitor Rpc intra-mPFC (0.025 μg/0.3 μL) to selectively block mPFC activity (Fig. 6a). At this dose, Rpc alone did not alter MC (Fig. 6b). However, it prevented the impairment in the 6-DOT when given in combination with SKF 38393 (0.1 mg/kg) (Fig. 6b; Supplementary Table 4). Importantly, intra-mPFC Rpc also prevented the high dose SKF-induced increase in PKA activity in the mPFC of double-injected mice (Fig. 6c). As a follow up step, to understand whether the inhibition of the mPFC could influence the PKA activity of the STR, we measured PKA phosphorylation in the STR of the same animals. Interestingly, intra-mPFC Rpc increased PKA substrate phosphorylation in double-injected mice, thereby restoring PKA activity in the STR (Fig. 6d).

Accordingly, we also found that systemic injection of SKF 38393 (0.1 mg/kg) together with the PKA agonist Spc in the STR rescued the impaired performance in the 6-DOT (Supplementary Fig. 6; Supplementary Table 4). The latter evidence further suggests that the high dose of SKF 38393 impaired WMC by activating PKA in the mPFC through the inhibition of the STR.

To confirm that that the impairing dose effect of SKF 38393 was due to the hyperactivation of the mPFC-STR pathway, we used an optogenetic approach by specifically blocking this pathway under the impairing dose of SKF 38393. Animals were infected with AAV2/2-hSyn-eNpHR 3.0-EYFP to transduce an inhibitory opsin (halorhodopsin) in the mPFC, and light stimulation was performed in the STR during the 6-DOT and under the impairing SKF dose (Fig. 7a). AAV expression in the mPFC and mPFC-STR terminals was assessed by immunofluorescence (Supplementary Fig. 7a). Interestingly, photoinhibition of the mPFC-STR pathway prevented the impairment induced by SKF 38393 0.1 mg/kg (Fig. 7b), without changing locomotor activity and exploratory behaviour (Supplementary Table 5). No effects of photoinhibition were found on vehicle treated mice; similarly, no effect of light was observed in SKF-treated animals infected with the empty halorhodopsin vector (pAAV-hSyn-EGFP). As expected, photoinhibition did not change the number c-Fos$^+$ cells in the mPFC (Fig. 7c, d), but it increased the number of c-Fos$^+$ cells in the STR, compared to the control group, suggesting a reactivation of the STR (Fig. 7e, f), in line with the results of the pharmacological experiments.

https://doi.org/10.1038/s41467-025-57788-5

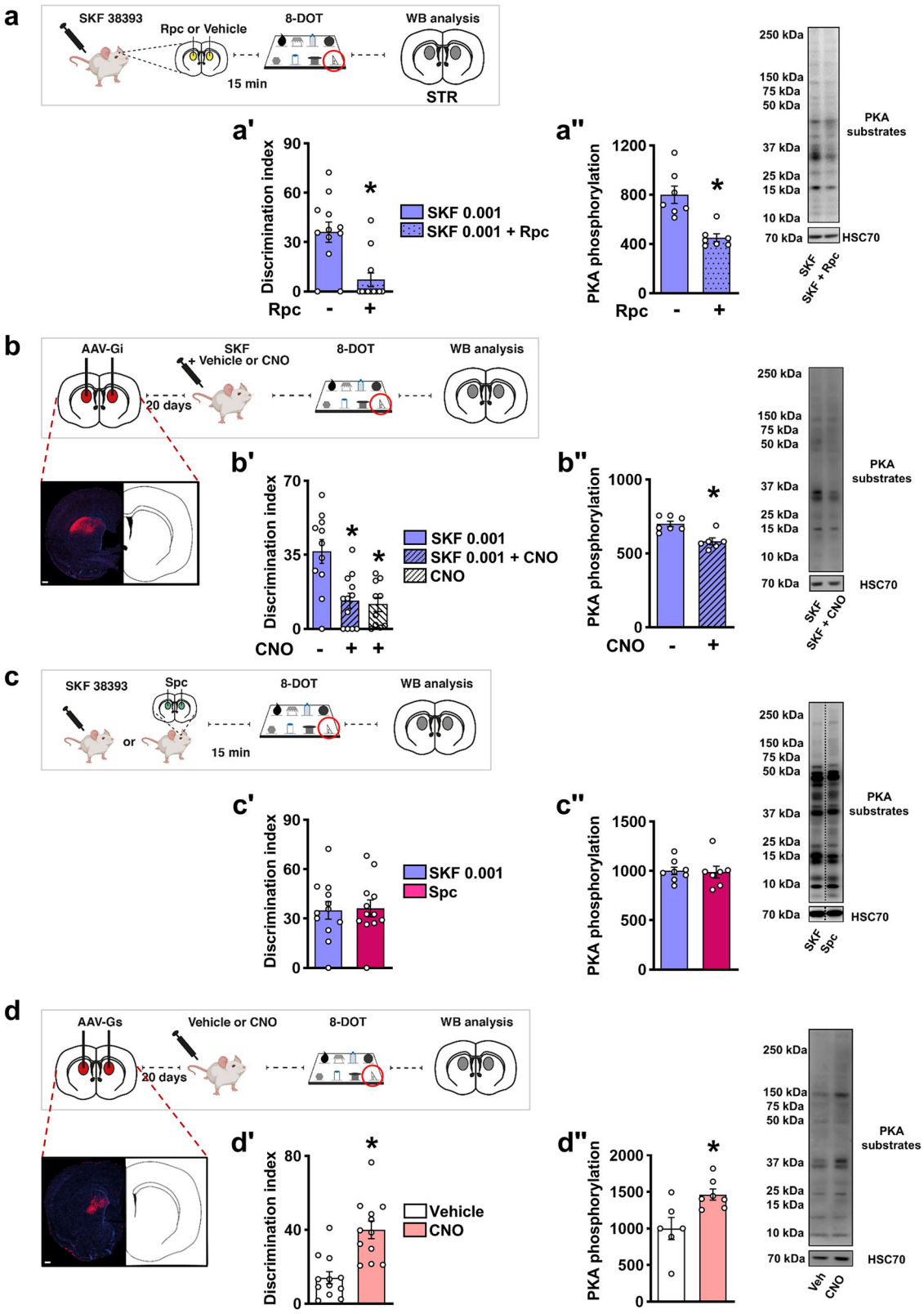

D1R activation in the cortex is known to regulate striatal activity through direct glutamatergic inputs[43,44]. Our data suggested that the hyperactivation of the mPFC activates an inhibitory mechanism in the STR, which has been shown to be mediated by GABAergic parvalbumin+ (PV^+) interneurons through mPFC glutamatergic inputs[43,44]. Accordingly, we found that the optogenetic inhibition of the mPFC-STR pathway reduced the number of double labelled $c\text{-}Fos^+/PV^+$ within the STR (Fig. 7g, h), suggesting that it acted by reducing the inhibitory tone in this region. No changes were observed in the total number of PV^+ cells in the STR (Supplementary Fig. 7b). To confirm this hypothesis, we used PV-Cre knock in mice, which express Cre recombinase in PV-expressing neurons[45], in order to selectively silence PV interneurons in the DMS by focally injecting the Cre-dependent inhibitory DREADD AAV-hSyn-DIO-hM4D(Gi)-mCherry.

https://doi.org/10.1038/s41467-025-57788-5

Fig. 5 | Inhibition of striatal D1R downstream signalling prevents the memory capacity increase mediated by SKF 38393, while its stimulation mimics the SKF-improving effects. a Schematic of the experimental design.Mice were administered systemically with 0.001 mg/kg SKF 38393 together with intra-striatal injection of vehicle or the cAMP antagonist (RP)-cAMPS (Rpc), tested in the 8 different objects test (8-DOT) and subsequently assayed for PKA phosphorylation in the striatum (STR). **a'** The discrimination index during the 8-DOT (One-way ANOVA: Treatment: $F_{1,22} = 15.187$; $p = 0.0008$). **a"** Representative immunoblot and quantification of PKA phosphorylation substrates (One-way ANOVA: Treatment: $F_{1,12} = 20.31$; $p = 0.0007$). **b** Schematic of the experimental design. Mice were infected with AAV2/5-CaMKIIa-HA-rM4D(Gi)-IRES-mCitrine (AAV-Gi) in the STR, injected withSKF 38393 0.001 mg/kg or CNO,tested in the 8-DOT and subsequently assayed for PKA phosphorylation. **b'** Effects of SKF 38393, CNO, or their combination on the discrimination index (One-way ANOVA: Treatment: $F_{2,30} = 10.54$; $p = 0.0003$, Tukey's post hoc) (**b"**) Representative immunoblot and quantification of PKA phosphorylation substrates (One-way ANOVA: Treatment: $F_{1,11} = 16.06$; $p = 0.0021$). **c** Schematic of the experimental design: mice were systemically administered with SKF 38393 0.001 mg/kg or with intra-striatal injection of vehicle or the cAMP agonist (Sp)-cAMPS (Spc). **c'** The discrimination index during the 8-DOT under SKF 38393 or Spc treatment (One-way ANOVA: Treatment: $F_{1,22} = 0.02$; $p = 0.8742$) (**c"**) representative immunoblot and quantification of PKA phosphorylation substrates (One-way ANOVA: Treatment: $F_{1,13} = 0.02$; $p = 0.8669$) were reported. **d** Schematic of the experimental design. Mice were infected with AAV2/5-CaMKIIa-HA-rM3D(Gs)-IRES-mCitrine (AAV-Gs) in the STR, injected with vehicle or CNO,,tested in the 8-DOT and subsequently assayed for PKA phosphorylation. **d'** Effects of vehicle or CNO in animals expressing AAV-Gs on the discrimination index (One-way ANOVA: Treatment: $F_{1,22} = 19.93$; $p = 0.0002$). **d"** Representative immunoblot and quantification of PKA substrates phosphorylation (One-way ANOVA: Treatment: $F_{1,11} = 8.15$; $p = 0.0156$). Data in bar charts are presented as mean values ± SEM. *p < 0.05 vs SKF or vehicle. Scale bars: 100 μm. Source data are provided as a Source Data file.

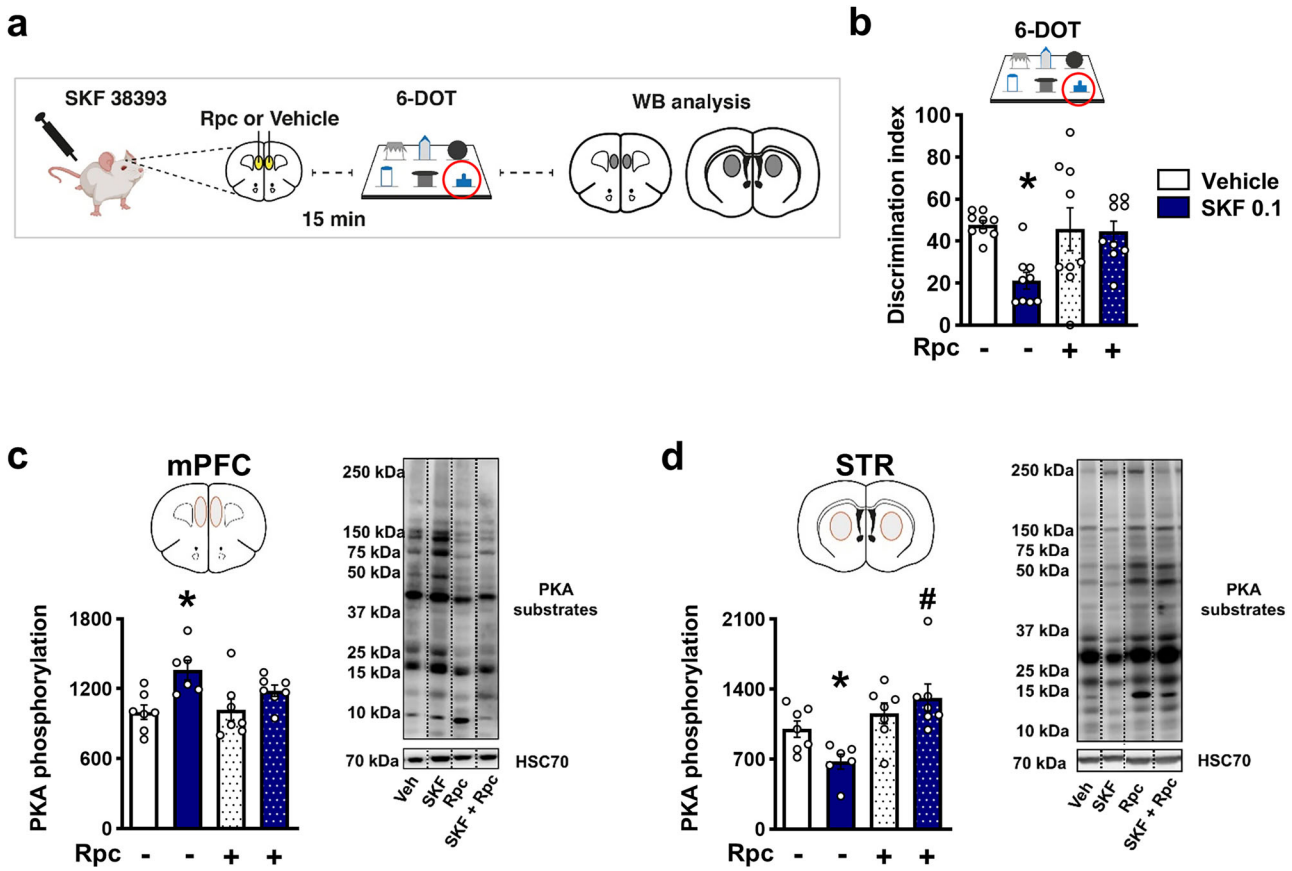

Fig. 6 | Inhibition of the D1R downstream signalling in the medial prefrontal cortex prevents the memory capacity impairment mediated by the high dose of SKF 38393. a Schematic of the experimental design. Mice were administered systemically with the impairing dose of SKF 38393 (0.1 mg/kg) or vehicle and injected locally in the medial prefrontal cortex (mPFC) with vehicle or the cAMP antagonist (RP)-cAMPS (Rpc, 0.025 μg/0.3 μl). The mice were then tested in the 6 different objects test (6-DOT) and subsequently assayed for PKA phosphorylation in both mPFC and striatum (STR) (red circles in the pictures). **b** Effects of the treatment with vehicle or SKF 38393 0.1 mg/kg or intra-mPFC of Rpc or the combination of both. Intra-mPFC Rpc alone did not change the performance in the 6-DOT, compared to vehicle. When given in combination with SKF, it prevented the impairing effects mediated by the high dose of SKF on WMC (One-way ANOVA: Treatment: $F_{3,32} = 4.23$; $p = 0.0126$, Tukey's post hoc). **c**, **d** Representative immunoblots and quantification of PKA substrates phosphorylation. Intra-mPFC Rpc suppresses the PKA substrates phosphorylation increase caused by the impairing dose of SKF 38393in the mPFC (c) (One-way ANOVA: Treatment: $F_{3,23} = 4.95$; $p = 0.0085$, Tukey's post hoc) and the hypoactivation of PKA in the STR of SKF (d) (One-way ANOVA: Treatment: $F_{3,23} = 6.640$; $p = 0.0022$, Tukey's post hoc). Data in bar charts are presented as mean values ± SEM. *p < 0.05 vs vehicle. #p < 0.05 vs SKF 0.1 mg/kg. Source data are provided in the Source Data file.

Before undergoing the 6-DOT, mice were treated with SKF (0.1 mg/kg) alone or in combination with CNO (1 mg/kg) (Fig. 8a). Mice injected with SKF-CNO showed a higher discrimination index (Fig. 8b, Supplementary Table 6) and increased c-Fos$^+$ cells in the DMS compared to control mice injected with SKF 0.1 or CNO alone (Fig. 8c, d). Of note, chemogenetic inhibition of striatal PV$^+$ neurons impaired performance in the 6-DOT, consistently with previous studies showing similar effects in the early phase of other striatal dependent tasks[46]. This result further strengthens the interpretation suggesting that the recruitment of PV$^+$ neurons to the task was mediated by high-dose SKF. Additionally, it supports the idea that preventing their activation mitigates the deleterious effects of high-dose SKF (Fig. 8e).

https://doi.org/10.1038/s41467-025-57788-5

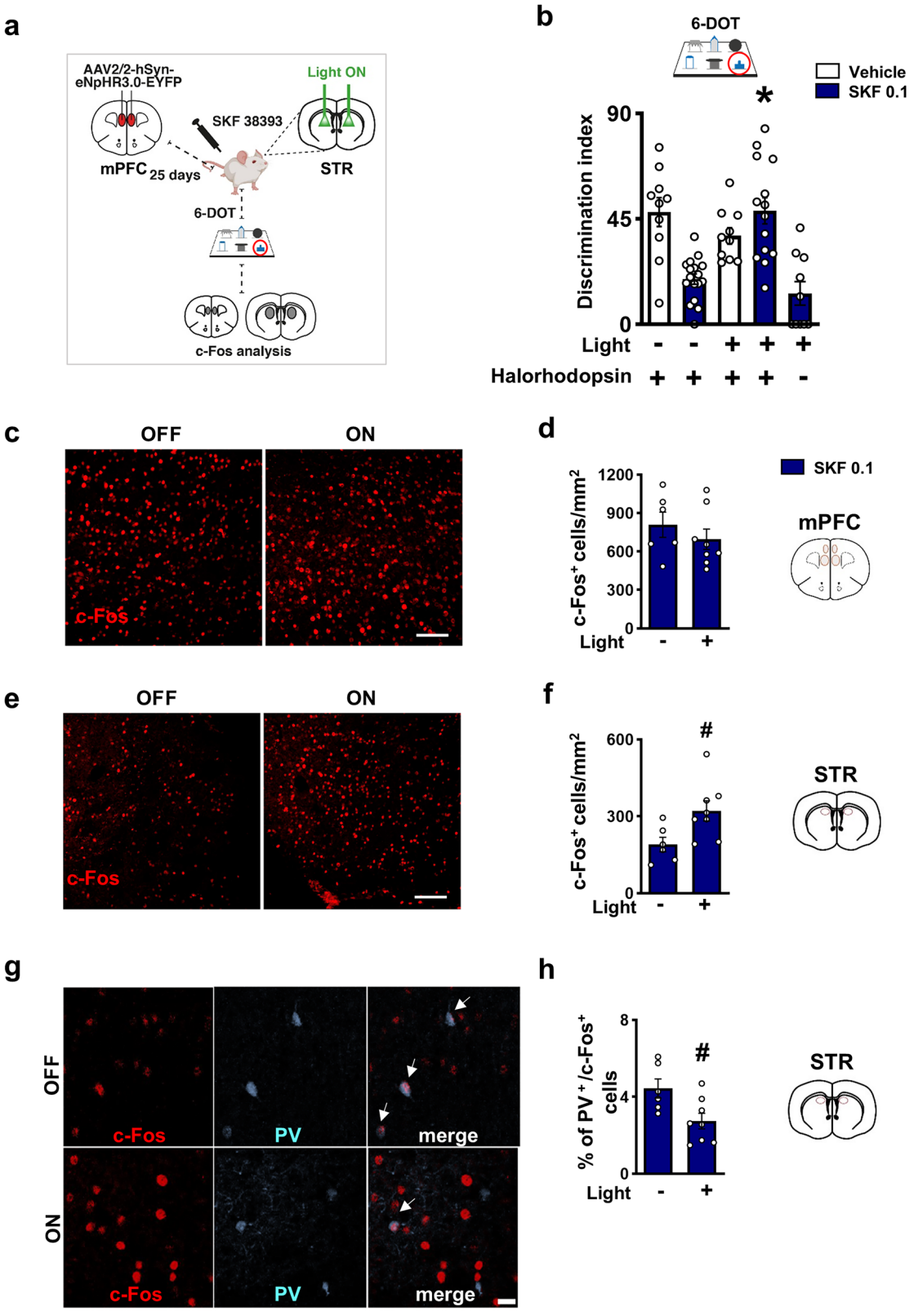

MC impairment in a pharmacological animal model of schizophrenia is rescued by low doses of SKF 38393

Symptomatic management of psychosis is accomplished using classic antipsychotics, such as the D2R antagonist haloperidol, which are effective in treating positive symptoms such as hallucinations. However, cognitive symptoms, such as reduced WMC, are not ameliorated by these treatments but often are even worsened, resulting in an unmet medical need. To test the translational potential of the improving dose of SKF 38393 to normal WMC, we used a pharmacological animal model of schizophrenia[47,48]. The model was made by sub-chronically injecting juvenile naïve mice with the non-competitive NMDA antagonist MK-801 (0.3 mg/kg)[49–51]. We then tested their memory in the 6-DOT (high load) and the 6-identical object test (6-IOT), which provides the same number of objects as the 6-DOT but

Fig. 7 | Optogenetic inhibition of the fronto-striatal circuit rescues the memory capacity impairment induced by the higher dose of SKF 38393 by decreasing Parvalbumin interneuron activation in the striatum. a Schematic of the experimental design. Mice were infected with AAV2/2-hSyn-eNpHR 3.0-EYFP or AAV2/2-hSyn-EGFP in the medial prefrontal cortex (mPFC) and fiber optics were implanted in the striatum (STR). Photoinhibition was activated after systemic administration of the impairing dose (0.1 mg/kg) of SKF 38393 and during the 6 different objects test (6-DOT). **b** Discrimination index of vehicle or SKF 38393 0.1 mg/kg injected mice with light OFF and under photoinhibition (light ON). The group treated with SKF 38393 0.1 mg/kg under photoinhibition increased the discrimination index compared to SKF 38393 light OFF and to SKF 38393 light ON without Halorhodopsin (One-way ANOVA: Treatment: $F_{4,54} = 11.13$; $p < 0.0001$; Tukey's post hoc). **c**–**f** c-Fos immunostaining and quantification of the number of c-Fos positive cells/mm^2 in the mPFC and STR in SKF 38393 0.1 mg/kg light OFF and light ON mice. The optogenetic inhibition did not change the number of c-Fos$^+$ cells in the mPFC (d) but increased it in the striatum (One-way ANOVA: Light: $F_{1,12} = 6.34$; $p = 0.0270$) (f). Scale bars: 100 μm. **g**–**h** Photoinhibition decreased the number of double-labelled Parvalbumin (PV$^+$) and c-Fos$^+$ neurons (One-way ANOVA: Light: $F_{1,12} = 7.0$; $p = 0.0209$). Arrows indicate double labelled PV$^+$/c-Fos$^+$ neurons. Scale bars: 25 μm. Data in bar charts are presented as mean values ± SEM. *$p < 0.05$ vs SKF #$p < 0.05$ vs Light OFF. Source data are provided in the Source Data file.

since they are all identical it requires a low MC (Fig. 9a). Sub-chronic MK-801 treatment did not affect performance in the 6-IOT (Fig. 9b), as MK-801-treated animals showed comparable levels in discrimination of the novel object as vehicle-treated animals. In contrast, they showed impairment in the 6-DOT, as shown by their reduced exploration of the novel object (Fig. 9c). These data suggest that MK-801-treated animals have a memory load-dependent impairment. Indeed, no effect was observed on locomotion during habituation or total exploration in the study phase (Supplementary Table 7), indicating that the impairment was not due to non-specific effects of the drug. After the behavioural assessment, MK-801 and vehicle-treated mice were split into four subgroups that were treated with vehicle, SKF 38393 (0.001 mg/kg), haloperidol (0.075 mg/kg, dose chosen based on ref. 31), or SKF 38393 and haloperidol, and retested in the 6-DOT or 6-IOT (Fig. 9a). We included a haloperidol-treated group since this antipsychotic drug is known to improve sensorimotor gating deficits but it has no pro-cognitive effect and a dose-dependent detrimental one[52]. By including a group treated with haloperidol and SKF 38393, we tested whether there was an interaction between the two drugs on behavioural performance. Based on our previous findings, we expected that haloperidol would affect novel object recognition in both low and high memory load conditions[31]. Results showed that the group that was pre-treated with MK-801 and then with vehicle was still impaired in the 6-DOT, suggesting that the defect lasted for days after ending the treatment (Fig. 9e). However, haloperidol, when given chronically, dramatically impaired performance in the 6-DOT in both vehicle and MK-801 pre-treated animals (Fig. 9e). Furthermore, it also affected locomotion during the habituation phase (Supplementary Table 8). We then tested the effects of chronic treatment with SKF 38393. We found that the D1R agonist fully rescued the performance of MK-801 pre-treated animals in the 6-DOT (Fig. 9e), without affecting locomotion or object exploration during the study phase (Supplementary Table 8), or the performance in the 6-IOT (Fig. 9d), suggesting that its improving effects were specific for the high memory load test.

Together, these findings provide the evidence that chronic administration of low doses of SKF 38393 rescues WMC deficits in an animal model of psychosis, without major side effects. Nevertheless, the beneficial effects of SKF 38393 were blocked by simultaneous administration of haloperidol (Fig. 9e).

Discussion

Several studies in rodents and primates report that D1R agonists exert an inverted-U shaped dose-response on cognitive functions. However, the underlying molecular mechanisms have remained elusive despite decades of investigation. This is partially due to the fact that the effects of these drugs have been independently analysed in the cortex and the STR, even if D1R activation in the cortex is known to regulate striatal activity through direct glutamatergic inputs.

In this work, using a behavioural procedure that permits studying WMC in rodents, we first asked whether and how we could expand WMC beyond its physiological limits using D1 agonists. The results showed that a low dose (0.001 mg/kg) of the D1R selective agonist SKF 38393 expanded MC in normal mice from 6 to 8 objects, increasing what is regarded as the highest memory load condition[20,21]. Using multiple approaches, we found that the beneficial effects of low doses of SKF 38393 on WMC are mediated by striatal activation of cAMP/PKA signalling. These results provide compelling experimental evidence of an intracellular pathway that can effectively enhance WMC beyond its normal limit. This set of data builds upon Goldman-Rakic's and Dash's observations[22,23] indicating that, under normal conditions, D1R activation in the mPFC is crucial for WM maintenance. Low doses of DA agonists lead to a supra-threshold increase in WM capacity by activating the cAMP/PKA pathway in the STR. However, our data clearly demonstrate that PKA activation is not an entirely negative mechanism for WM; it is only negative for the mPFC. In fact, the activation of cAMP/PKA signalling in the striatum is a necessary and sufficient condition for MC expansion. This opens the way to the study of selective drugs and brain-targeted therapies. These findings align with pre-clinical and clinical studies on the effects of cortical and striatal phosphodiesterase inhibitors (which increase cAMP levels) in regulating working memory[53–55]. However, they challenge the traditional view that PKA activation in D1- and D2-expressing striatal neurons exerts opposing effects on behaviour.

While literature shows a dissociation between these pathways under specific conditions, emerging evidence highlights the animal's motor state as a key determinant of whether one or the other striatal pathway is activated[56–58]. This is in line with findings that dopamine release can synchronously activate both pathways, which may share behavioural functions[34,59].The role of D1/D2-SPNs co-expressing medium spiny neurons (SPNs) further complicates this view. Despite their low density, their contribution to regulating complex behaviours has only recently been explored, mainly in locomotion[58], with no evidence on their involvement in working memory. Future studies should investigate how these cell-type-specific pathways are regulated by cortical inputs and their roles in stimulus encoding or memory maintenance in normal and pathological conditions, such as neuropsychiatric disorders.

During aging and neuropsychiatric disorders, as well as psychosis, reduced WMC or impaired WM are associated with abnormal DA or D1R expression[60]. Here we also show that a sub-chronic treatment with low doses of SKF 38393 rescued the WMC defect in the pharmacological (MK-801) model, while haloperidol had detrimental effects. These data are consistent with other findings showing that directly targeting the D1R[61–63] or its downstream pathway (cAMP/PKA) (for review see ref. 64) is an effective therapeutic strategy to rescue cognitive deficits in schizophrenia. Indeed, there was not a general impairment in cognition in MK-801-treated mice, as performance in low memory load conditions (the 6-IOT) was normal. At the same time, the impaired performance in the 6-DOT was not ascribable to non-specific signs of motor impairment or lack of interest in novelty, as no changes were observed in these parameters. These results are in line with previously reported examples of impairment in the odour span task[65]. Therefore, this mouse model, as well as schizophrenic patients[4], can normally perform tests that have a low number of objects to remember, but they fail when WMC is loaded with additional elements. These findings pave the way for the

https://doi.org/10.1038/s41467-025-57788-5

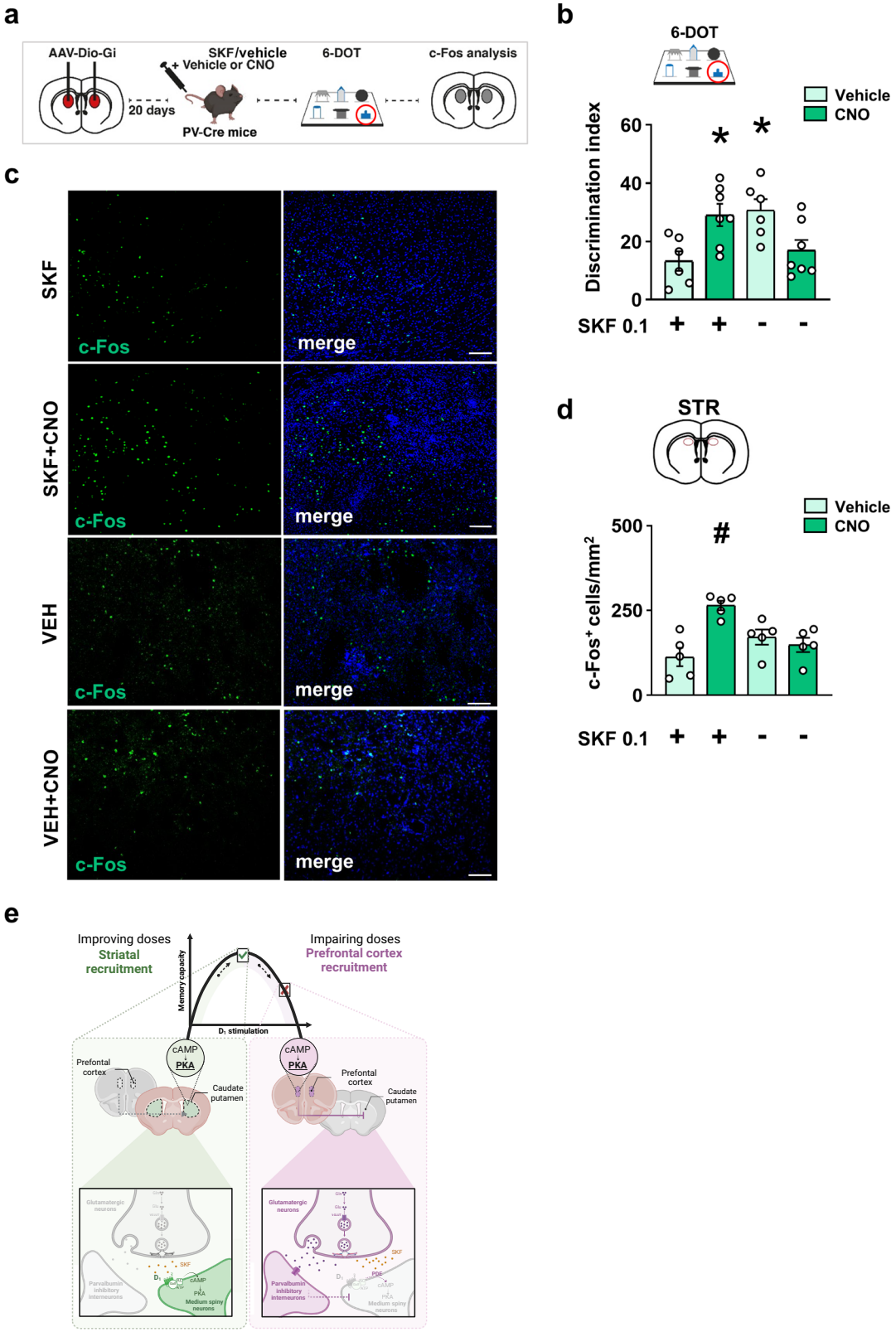

generation or discovery of models that can be used to test the effects of classic and alternative treatments for WMC deficits associated with schizophrenia.

Our results, however, once again confirm that increasing the dose of SKF 38393 (0.1 mg/kg) impairs performance in the memory test and reduces WMC, in line with an inverted-U dose-response of D1R agonists previously reported in both rodents and primates using similar dose-ranges of D1R agonists (low: 0.00001–0.0001 mg/kg vs. high: 1–6 mg/kg[14,1519]). Previous studies have explored possible mechanisms at local, mPFC, and STR levels. Using D1 agonists with different functional selectivity, dose-dependent effects not only at the single-cell level in the PFC but also at the neuronal ensemble level, that might support decision-making during task performance, have been reported[25,26]. Similar results in monkeys showed that

Fig. 8 | Selective inhibition of striatal Parvalbumin-positive cells in PV-Cre mice rescues the memory capacity impairment induced by the higher dose of SKF 38393. a Schematic of the experimental design. PV-Cre mice were infected with AAV-hSyn-DIO-hM4D(Gi)-mCherry in the striatum (STR). Before undergoing the 6 different objects test (6-DOT), mice were treated with SKF 0.1 mg/kg together with vehicle or CNO 1 mg/kg. **b** The discrimination index in double injected mice (SKF + CNO), but not of the CNO group (vehicle + CNO), was similar to that of the control group (Vehicle + Vehicle) (Two-way ANOVA: Pre-treatment SKF 0.1/ vehicle: $F_{1,22} = 0.07$; $p = 0.7807$; Treatment CNO/ vehicle: $F_{1,22} = 0.5$; $p = 0.4806$; Pre-treatment x Treatment: $F_{1,22} = 15.95$; $p = 0.0006$, Tukey's post hoc). **c** Representative images of immunofluorescence staining using an anti-c-Fos antibody and (**d**) relative quantification. CNO-SKF injected animals show increased c-Fos$^+$ cells in the STR compared to control mice injected with SKF 0.1 or Vehicle (Veh) (Two-way ANOVA: Pre-treatment SKF 0.1/ vehicle: $F_{1,16} = 8.8$; $p = 0.0090$; Treatment CNO/ vehicle: $F_{1,16} = 1.7$; $p = 0.2007$; Pre-treatment x Treatment: $F_{1,16} = 16.26$; $p = 0.0010$, Tukey's post hoc). Scale bars: 100 μm. **e** Graphical abstract of the proposed mechanism. The memory enhancing effects of D1 agonists are regulated by the recruitment of cAMP/PKA in the striatum. The memory impairing effects of a high dose of D1 agonists are due to cAMP/PKA activation in the medial prefrontal cortex, which leads to a recruitment of GABA interneurons in the dorsomedial striatum, preventing its activation. Created in BioRender https://BioRender.com/x47z499. Data in bar charts are presented as mean values ± SEM. *$p < 0.05$ vs SKF + Vehicle; #$p < 0.05$ vs all groups. Source data are provided in the Source Data file.

population coding in the PFC microcircuitry is governed by different cell types[66]. On the other hand, the results of the phosphoproteomic analysis highlighted how, through simple manipulation of the dose of dopaminergic agents, it is possible to engage different molecular players that act antagonistically at the level of the striatum.

We expanded on these observations by studying the effects at the fronto-striatal circuit level. The pro-cognitive dose of SKF activated all D1R downstream signalling pathways, which are known to feed-forward the direct striatal pathway and consequently affect behaviour. The fact that the same high dose of the drug that inactivates the STR also activates the mPFC suggests a mechanism of subcortical-to-cortical control shift upon excessive D1R stimulation. This finding is in line with previous data showing that striatal neurons are more responsive than mPFC neurons to DA stimulation[67]. The recruitment of D1R in the mPFC during the WM delay is necessary for memory maintenance in WM tasks[68]. However, the hyperactivation of cAMP/PKA as a consequence of D1R hyperstimulation or by direct infusion of cAMP agonists (Spc) into the mPFC[12,18,69] has been reported to impair cognition. Accordingly, the impairment was rescued by a cAMP/PKA inhibitor (Rpc) but not by an inhibitor of Protein Kinase C (PKC)[13]. In line with these findings, we report that the same impairing dose of SKF inhibited the activation of cAMP/PKA pathway in the STR and did not change the number of c-Fos$^+$ striatal cells, suggesting that the recruitment of the cAMP-PKA in the mPFC disengaged the STR. This conclusion is supported by the evidence that the impairing effects of SKF 38393 were rescued by the activation of the cAMP/PKA pathway in the STR by preventing cortical activation of cAMP/PKA.

Based on this evidence, we tested the hypothesis that the impairing dose of SKF 38393 disengages the STR by activating glutamatergic neurons projecting from the mPFC to the STR, which are known to exert feed-forward inhibition via activation of PV interneurons. PV interneurons are fast-spiking (FSIs) neurons, exclusively targeting nearby SPNs, forming strong synapses on their proximal somatodendritic regions, and likely sharing common excitatory inputs[70]. Chemogenetic inhibition of PV$^+$ striatal neurons or optogenetic inhibition of the mPFC-STR circuit rescued the memory impairment induced by a high dose of SKF 38393. These findings suggest that PKA activation in the cortex is detrimental to memory, but this effect is mediated at the circuit level, involving cortico-striatal recruitment of GABAergic interneurons, rather than being purely cortical.

Although, beyond the scope of this work it is interesting to speculate on the mechanisms through which prefrontal cAMP/PKA activation might lead to PV neuron recruitment in the striatum. Cortical PKA has been reported to act downstream of receptor blockade, enhancing synaptic transport and stability of glutamatergic NMDA receptors, thereby mediating physiological and pathological responses, such as excitotoxicity or synaptically released glutamate[71]. Striatal PV neurons receive direct cortical glutamatergic inputs and are readily activated by cortical stimulation. Notably, Mallet and colleagues showed that FSIs respond to high-frequency trains of suprathreshold cortical stimulation, with spike frequency increasing as the stimulating current exceeds the threshold. This suggests that the inhibitory feed-forward loop is activated only with suprathreshold mPFC activation. Thus, the high dose of SKF 38393, by recruiting cAMP/PKA signalling in the mPFC, might mimic this suprathreshold cortical stimulation[72].

Similarly, it is tempting to speculate about the functional significance of this cortico-striatal mechanism of top-down control. Intense dopaminergic activation, as seen with higher doses, is associated with "biological alertness"[23] or excitotoxicity, triggering cAMP/PKA pathway activation in the mPFC. This activation may enable the mPFC to regain control over subcortical nuclei, particularly the STR, by inhibiting the direct pathway through inputs reaching inhibitory neurons. This mechanism could facilitate the flexible allocation of cognitive resources, allowing the brain to adapt and prioritise between goal-directed behaviours and higher cognitive functions, such as expanded working memory capacity, as needed.

In conclusion, data produced thus far suggests that WM can be improved by D1 not only in terms of duration of retention interval but also in terms of capacity, and this latter mechanism is governed by the activation of cAMP/PKA signalling in the striatum. Conversely, the activation of the same pathway in the cortex prevents the striatal-mediated expansion of WMC through the recruitment of inhibitory GABAergic interneurons in the striatum. These results could not have been anticipated based on the theories available so far and fill an important gap in the mechanisms regulating WMC. Additionally, they reinforce the need to approach dopaminergic agents using systems pharmacology. This strategy considers the response to a drug not simply as a result of one specific drug-receptor interaction, but as the outcome of brain network interactions which, in turn, control the activation of intracellular signalling cascades regulating complex behaviours.

Methods

Subjects

All pharmacological and optogenetic experiments were performed in 10–16-week-old CD1 outbred male adult mice (Charles River, Italy), except experiments in Fig. 8 which were performed using transgenic B6;129P2-Pvalb $^{tm1(cre)Arbr/J}$ male mice aged 3 months (Jackson Laboratory, here called PV-Cre mice[45]). Sub-chronic treatments in the animal model of schizophrenia were performed on juvenile CD1 outbred male mice (4–5 weeks old, Charles River) to mimic the human onset of psychosis. All mice were housed in groups of 3–5 subjects in standard breeding cages placed in a rearing room at a constant temperature (22 ± 1 °C) and maintained on a 12 h light/dark cycle with food and water available ad libitum. All procedures were performed in strict accordance with the European Communities Council directives and Italian laws on animal care (446/2015 PR; 781/2019 PR).

Different objects test/identical object test (DOT/IOT)

Animals were acutely injected, isolated in a waiting cage, and then submitted to the DOT/IOT as previously described[2]. Briefly, mice underwent a habituation trial (10 min) in an empty open field (35 × 47 × 60 cm). After 1 min in the waiting cage, they were subjected to the study phase, during which they were allowed to explore the

https://doi.org/10.1038/s41467-025-57788-5

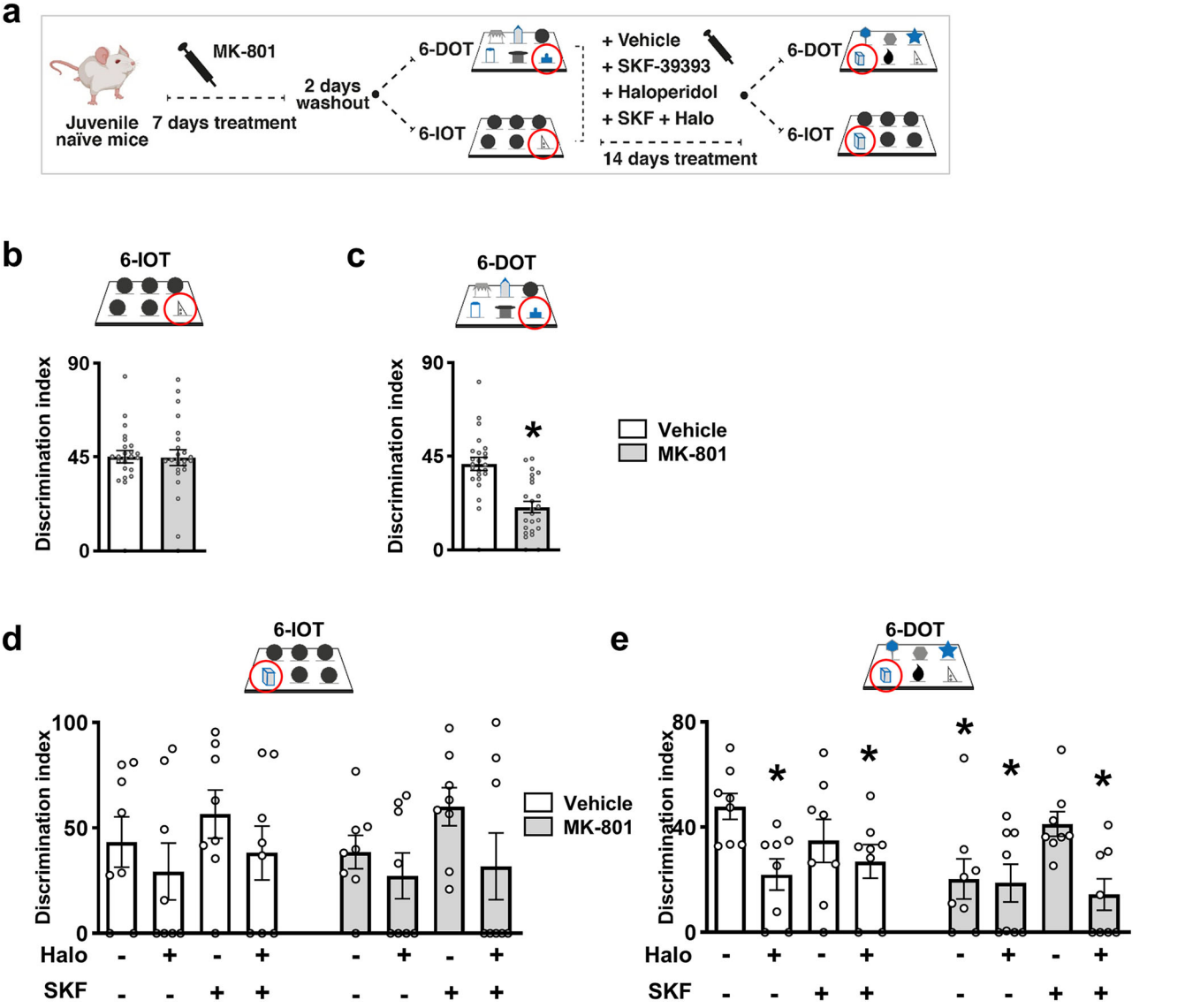

Fig. 9 | SKF 38393 rescues memory capacity impairment in a pharmacological animal model of schizophrenia. a Schematic of the experimental design of MK-801 treatment. Mice were treated with vehicle or MK-801 for 7 days, followed by two days of wash-out. They were then tested in the 6 different objects test (6-DOT) or 6 identical objects test (6-IOT). The day after, mice were divided into four sub-groups: vehicle, haloperidol, SKF 38393, and haloperidol plus SKF. The treatment lasted 14 days. On the last day, they were retested in the 6-DOT or 6-IOT under drug. **b** Effects of sub-chronic treatment of MK-801 (0.3 mg/kg) on the discrimination index during the 6-IOT (One-way ANOVA: Treatment: $F_{1,46} = 0.009$; $p = 0.9239$) and **(c)** the 6-DOT (One-way ANOVA: Treatment: $F_{1,46} = 24.91$; $p < 0.0001$). MK-801 specifically impaired memory capacity in high but not in low memory load condition. **d** Effects of haloperidol (Halo) (0.075 mg/kg), SKF 38393 (0.001 mg/kg), and haloperidol in combination with SKF on the discrimination index during the 6-IOT (Two-way ANOVA: Pre-treatment: $F_{1,56} = 0.08$; $p = 0.7777$; Post-treatment: $F_{3,56} = 2.33$; $p = 0.0832$; Pre-treatment x Post-treatment: $F_{3,56} = 0.06$; $p = 0.9775$) and **(e)** 6-DOT (Two-way ANOVA: Pre-treatment: $F_{1,56} = 4.06$; $p = 0.0486$; Post-treatment: $F_{3,56} = 3.93$; $p = 0.0128$; Pre-treatment x Post-treatment: $F_{3,56} = 2.48$; $p = 0.0700$, Tukey's post hoc). Haloperidol, when given chronically, dramatically impaired performance in the DOT in both vehicle and MK-801 pretreated animals. SKF rescued memory capacity impairment but did not prevent the impairing effects of haloperidol. Data in bar charts are presented as mean values ± SEM. *$p < 0.05$ vs vehicle. Source data are provided in the Source Data file.

objects. During the study phase, animals explored 6 identical objects (6-IOT), 6 different objects (6-DOT), or 8 different objects (8-DOT), corresponding to low, high, and overload memory conditions, respectively. They were allowed to explore the objects until they had accumulated 35 s of exploration time for each different object, which corresponded to 35 s, 210 s, and 280 s for the 6-IOT, 6-DOT, and 8-DOT, respectively. To collect the aforementioned exploration time, a maximum of 5, 10, and 15 min was allowed. During the test phase, one of the objects was replaced with a new one, while the others were replaced with identical copies of the original object, and animals were allowed to explore them for 5 min. Object exploration was defined as the time in which the nose of the animal was directed towards the object (<2 cm distance). Animal behaviour was recorded using a video-tracking system (Any-maze, Stoelting, USA) and analysed by trained observers, blind to the treatment. Results were expressed as a discrimination index, i.e., time spent exploring the new object as a percentage of the total exploration time. It was calculated using the following formula: [(New object exploration/Σ objects exploration) * 100]. The total distance travelled during the habituation phase and total objects exploration during the study phase were also used for the statistical analysis. A part of the mice was sacrificed immediately after completing behavioural tests by cervical dislocation for biochemical analysis of tissues (Western blot for PKA substrates) or they were perfused one hour after completing the task with phosphate-buffered

saline (PBS pH 7.4) for histological analysis (c-Fos counting). The remaining part was not used for further experiments.

Drugs

All drugs were purchased from Sigma Aldrich (Milan, Italy) except for CNO (Hello-Bio). SKF compounds (SKF 38393 and SKF 83822) and were dissolved in 0.9% saline and injected 15 min before initiating the behavioural tests (intraperitoneally ip). SCH 23390 was dissolved in 0.9% saline and injected 30 min before tests (ip). Rpc and Spc were dissolved in PBS and injected 20 min before tests (5 min before SKF 38393, intra-brain). CNO was dissolved in water and injected 30 min before tests (ip). MK-801 was dissolved in 0.9% saline (ip). We referred to "vehicle" as the solution in which each compound was dissolved.

Phosphoproteomic analysis

Mice were injected with vehicle, SKF 0.001 or SKF 0.1 mg/kg. After 15 min, they were tested in an empty open field for 30 min and then were immediately sacrificed by cervical dislocation and the STR rapidly dissected. Tissue lysis was performed by adding SDC lysis buffer containing 4% (w/v) SDC, 100 mM Tris -HCl (pH 8.5). Samples were immediately boiled at 95 °C for 5 min and sonicated in a bioruptor for 10 cycles at high intensity, 30 s on/30 s off. The protein concentration was then quantified using the BCA assay. Phosphoproteome preparation was performed by the EasyPhos workflow, as previously described[73]. Briefly, equal protein amount (>750 µg) was diluted in 750 µl of ACN and 250 µl of EP enrichment buffer containing 36% TFA and 3 mM KH_2PO_4. Samples were mixed at 2000 × *g* for 30 s to clear precipitates, centrifuged at 20,000 × *g* for 15 min and transferred to a 2 ml deep-well plate. To enrich phosphosites, TiO2 beadswere resuspended in EP loading buffer containing 80% ACN and 6% (v/v) TFA at a ratio of 12:1 (beads:protein) per sample, incubated for 5 min at 40 °C, by shaking at 2000 rpm and the beads were then pelleted at 2000 × *g*, 1 min. The supernatants (non-phosphosites) were discarded and the beads were washed twice in 500 µl of EP wash buffer consisting of 60% ACN and 1% TFA and then transferred to clean tube. Four additional washes with EP wash buffer were performed, mixing at 2000 rpm for 3 s. After washing, beads were resuspended in 75 µl of EP transfer buffer (80% ACN, 0.5% acetic acid), transferred on top of C8 stage tips (double layer), and spun to dryness at 1000 × *g*, 5 min. Phosphopeptides were eluted into PCR tubes with 30 µl of EP elution buffer (200 µl of NH_4OH and 800 µl of 40% can). Samples were concentrated immediately in a SpeedVac at 45 °C, 20 min. Meanwhile, SDB-RPS StageTips (triple layer) were equilibrated using (i) 100 µl ACN, (ii) 100 µl 30% methanol/1% TFA, and (iii) 150 µl 0.2% TFA. SDBRPS loading buffer (1% TFA in isopropanol) was added to the samples which were loaded onto the equilibrated SDB-RPS StageTips. After washing the StageTips with (i) 100 µl 1% TFA in EtOAc, (ii) 100 µl of 1% TFA in isopropanol, and (iii) 150 µl of 0.2% TFA, the phosphopetides were eluted into clean PCR tubes with a buffer containing 60% ACN and 5% NH_4OH. After SpeedVac at 45 °C for 30 min, phosphopetides were resuspended in 10 µl of 2% can/0.1% TFA.Phosphopeptides were analyzed by liquid chromatography tandem mass-spectrometry (LC-MS/MS) analysis consisting of a NanoLC 1200 coupled via a nano-electrospray ionisation source to the quadrupole-based Q Exactive HF benchtop mass spectrometer[74]. Peptide separation was carried out according to their hydrophobicity on a PicoFrit column, 75 µm ID, 8 Um tip, 250 mm bed packed with Reprosil-PUR, C18-AQ, 1.9 µm particle size, 120 Angstrom pore size (New Objective, Inc., cat. PF7508-250H363), using a binary buffer system consisting of solution A (0.1% formic acid) and B (80% acetonitrile, 0.1% formic acid). Total flow rate was 250 nl/min.After sample loading, the run consisted of a series of linear gradients of buffer B (5% to 25% for 85 min, 25% to 43% for 35 min, 43% to 60% for 35 min), with a final 10 min step to reach 90%, which was maintained for 5 min.

MS spectra were acquired using 3E6 as an AGC target, a maximal injection time of 120 ms and a 60,000 resolution at 200 m/z. The mass spectrometer operated in a data dependent Top10 mode with subsequent acquisition of higher-energy collisional dissociation (HCD) fragmentation MS/MS spectra of the top 10 most intense peaks. Resolution for MS/MS spectra was set to 15,000 at 200 m/z, AGC target to 1×10^5, max injection time to 120 ms, and the isolation window to 1.6 Th. The intensity threshold was set at 3.3E5 and Dynamic exclusion at 40 s. All acquired raw files were processed using MaxQuant (1.6.2.10), implemented with Andromeda search engine. For protein assignment, spectra were correlated with the Uniprot Mouse (v. 2021), including a list of common contaminants. Searches were performed with tryptic specifications and default settings for mass tolerances for MS and MS/MS spectra. Perseus software (1.6.2.3) was used and first filtered for contaminants and reverse entries as well as proteins that were only identified by a modified peptide. Then, intensity values were filtered for the sites that have localisation probability >0.75. The values were grouped and filtered for minimum valid number (minimum 3 in at least one group). The intensities were normalised by subtracting the median intensity of each sample. Missing values were replaced by random numbers that were drawn from a normal distribution. Differential abundance of phosphosites analysis was performed using the ANOVA test with a threshold of FDR < 0.05. For enrichment analysis, we used the R Studio software (version 4.1.2), and differential analysis of phosphosites abundance was carried out using LIMMA (version 3.50.0)[75]. Overregulated phosphosites with statistically significant abundance (Adjusted $P < 0.05$) were filtered in both improving dose versus vehicle, impairing dose versus vehicle, and improving dose versus impairing dose comparisons, after which protein enrichment analysis was performed. Webgestalt[76] and g:Profiler[77] webtools were used to determine the most enriched Gene Ontology terms and pathways. Heat maps for the 50 most variable phosphosites were generated using the pheatmap R package (version 1.0.12) and the Venn Diagram was generated using VennDiagram R package (version 1.2.2).

AAV preparation

Plasmids for DREADDs and optogenetic experiments were purchased from Addgene. For DREADDs experiments we used pAAV-CaMKIIa-HA-rM3D(Gs)-IRES-mCitrine (#50468) and pAAV-CaMKIIa-HA-hM4D(Gi)-IRES-mCitrine (#50467). For optogenetic experiments we used pAAV-hSyn-eNpHR 3.0-EYFP (#26972) and pAAV-hSyn-EGFP (#2906). For PV-Cre experiments we used pAAV-hSyn-DIO-hM4D(Gi)-mCherry (#44362). Plasmids were amplified and purified using EndoFree Plasmid Mega Kit (Qiagen) following the manufacturer's instructions. AAVs were assembled by the TIGEM AAV Vector Core. The AAV serotypes had the following titres (GC/ml): 1.4×10^{12} for AAV 2/5-CaMKIIa-HA-rM3D(Gs)-IRES-mCitrine, 2.1×10^{12} for AAV 2/5-CaMKIIa-HA-hM4D(Gi)-IRES-mCitrine, 8.4×10^{12} for AAV 2/2-h-SYN-eNpHR3.0-EYFP and 2.4×10^{13} for AAV-hSyn-DIO-hM4D(Gi)-mCherry.

Surgery

For surgical procedures, the animals were anesthetized with a combination of tiletamine/zolazepam (80 mg/kg) and xylazine (10 mg/kg) and positioned on a stereotaxic apparatus (Stoelting, USA). The surgical procedure for cannula implantation has been previously described[78]. In brief, mice were implanted bilaterally with 7-mm-long bilateral stainless steel cannulae. The stereotaxic coordinates used were: antero-posterior (AP) + 1.1 mm, mediolateral (ML) ± 1.5 mm, dorsoventral (DV) − 1.5 mm for the STR, and AP + 2.0 mm, ML ± 0.5, DV ± −2.5 for the mPFC relative to bregma, according to the mouse brain atlas of Franklin and Paxinos[79]. Guide cannulae were secured in place with dental cement. Mice were then allowed to recover for 7 days after surgery. The injector was 8-mm-long. Injection volume was 0.8 µL for the STR and 0.3 µl for the PFC. At the end of the experiment, animals were sacrificed, brains removed, and the injection sites were

verified by Western blot analysis (PKA substrates analysis) or by immunofluorescence for DREADDs/optogenetic experiments.

For virus injection, the surgical procedure was previously described[32]. In brief, the anesthetized animals were secured on the stereotaxic apparatus, the skull surface was exposed and small craniotomies were performed at the coordinates of interest. The DREADDS injection was made in the STR at the following coordinates: AP + 1.1 mm, ML ± 1.5 mm, DV − 1.5 mm relative to bregma. For optogenetics, the AAV injection was made at the following coordinates: AP + 2, ML ± 0.5, DV - 2.5. Injection volume was 0.8 µl for the STR and 0.5 µl for the PFC. For fibre optic implantation, during the same surgery, one or two 200 µm core (0.39 NA) optic fibres were implanted at the coordinates: AP + 1.1, ML ± 1.6, DV - 3.15 AP. Two screws were fixed on the skull to ensure implant stability. Optic fibres were fixed in place with dental cement (Meliodent, Heraeus).

Light stimulation protocol for optogenetics experiments

Four to five weeks post-AAV injection, mice underwent the behavioural testing and light stimulation protocols. Before starting the behavioural test, the implantable fibres were coupled to a 120-mW, 532-nm diode pumped solid-state laser (Laserlands, PRC) using a one-input one-output rotary joint (Thorlabs, USA) connected to a bifurcated fibre bundle (Thorlabs, USA). Power output from the tip of the bifurcated fibre bundle was about 11–12 mW. Immediately after the injection of impairing dose of SKF or vehicle, mice were photostimulated (light ON) or not (light OFF) for the entire test, from habituation to test phase.

Western blotting

Mice were sacrificed through cervical dislocation and their brains were collected. The whole STR and mPFC were then rapidly dissected. Tissues were homogenised in RIPA buffer (25 mM Tris-HCl pH 7.4; 150 mM NaCl; 100 mM EDTA; 1% Triton X100; cocktails of proteases and phosphatase inhibitor) and then centrifuged at 13,200 *g* for 15 min. After protein quantification (Bradford, BioRad), 40 µg of protein were loaded on an SDS-polyacrylamide gel. The proteins were transferred to PVDF membranes and blocked with 5% BSA in TTBS. Membranes were incubated with primary antibodies: Phospho-PKA Substrate (Cell Signalling #9624), PKA C-alpha subunit (Santa Cruz Biotechnology #sc-28316), or Hsc70 (Enzo Life Sciences #ADI-SPA-819) as a loading control, followed by incubation with the appropriate secondary antibody (rabbit or mouse) (BioRad). Immunoreactivity was detected by chemiluminescence (Millipore). The PKA catalytic subunit was expressed as percentage relative to the control, to correct for any differences between different gels (due for example to recycling of primary antibodies or time to ECL exposure). The Phospho-PKA Substrate was expressed as the sum of percentage relative to the control for each band.

AAV expression verification

For DREADDs experiments, after rinsing in 1x PBS, brain sections were incubated in blocking solution made of 5% normal goat serum (NGS) and 0.3% Triton X-100 in PBS for 1 h. The blocking solution was then removed and replaced with the primary antibody solution made of 1% NGS, 0.3% Triton X-100, and rabbit anti-HA tag antibody (#3724; Cell Signalling) diluted 1:500 overnight at 4 °C. Sections were washed three times in 1x PBS and then incubated for 2 h at room temperature with the secondary antibody solution made with 1% NGS, 0.3% Triton X-100, and goat-anti-rabbit Alexa Fluor 647 (Merck Millipore) diluted 1:300 in 1x PBS. After three washes with 1x PBS, sections were incubated for 10 min with 4′,6-diamidino-2-phenylindole (DAPI), for nucleic acid staining, at room temperature and then washed three times with 1x PBS. Finally, sections were mounted on microscope glass slides and covered with a coverslip with Mowiol (4-88; Sigma Aldrich). Control sections, which had not been exposed to the primary antibody, were processed in parallel. Images of slices were acquired using an Axioscan 7 microscope (Zeiss). Only mice expressing the reporter in the expected location were included in the statistical analysis.

For the optogenetics experiment, the EYFP and EGFP reporters wereused to verify AAV infection.

Immunofluorescence analyses

One hour after the test, in order to ensure c-Fos protein expression, mice were deeply anaesthetized and transcardially perfused with 1x PBS followed by 4% paraformaldehyde (PFA; Sigma Aldrich). Brains were collected and post-fixed for 24 h in PFA and passed in a 30% sucrose solution. 30 µm coronal slices were obtained using a cryostat and stored in PBS and sodium azide (0.02%) at 4 °C until histological processing. Three free-floating sections *per* animal were chosen.

After rinsing in 1x PBS, brain sections were incubated for 1 h in a blocking solution made of PBS, 0.3% Triton X-100, and 5% NGS. Blocking solution was then removed and slices were incubated overnight at 4 °C with a solution containing anti-c-Fos antibody (226017; Santa Cruz Biotechnology; 1:1000), PV antibody (GTX132759; Genetex; 1:500), or D1R antibody (SC33660; Santa Cruz Biotechnology; 1:200). The day after, sections were washed three times in PBS and then incubated for 2 h with appropriate secondary antibodies diluted 1:300 in PBS containing 0.3% Triton X-100 and 1% NGS. After three washes with 1x PBS, sections were incubated for 10 min with DAPI.

Finally, sections were mounted on microscope glass slides and covered with a coverslip with a Mowiol (4-88; Sigma Aldrich) solution. Control sections, which had not been exposed to the primary antibody, were processed in parallel. Images (20x or 60x magnification) were acquired using a Nikon Eclipse. The number of $D1R^+$ spots, $c\text{-}Fos^+$, PV^+, double labelled $c\text{-}Fos^+/PV^+$ or $cFos^+/D1R^+$ cells, were counted with Qupath 0.5.1, as previously described[32]. In brief, for each scanned slice, a region of interest (ROI) was selected based on the analyzed brain region. A positive cell detection tool was then used to identify cells positive for the markers of interest, and when necessary, a tool was applied to detect cellular colocalization and perform subcellular cell detection. Specifically, we sampled the STR considering the following anteroposterior coordinates relative to the bregma (according to ref. 79) from 1.18 to 0.38. Sections from each experimental group (vehicle 6-DOT, vehicle 8-DOT, SKF 0.001 8-DOT, SKF 0.01 6-DOT, or light ON, light OFF) were matched for each coordinate. Cell numbers from each section were counted within two different subregions, representative of dorsolateral and dorsomedial STR (DLS, DMS), as reported in the schemes of the main figures (Fig. 2b). The number of cells of each subregion were averaged and normalised on area (mm^2). Similarly, for the mPFC, we counted two different subregions (Cg and PrL/IL) relative to the bregma (according to ref. 79) from 1.98 to 1.54. Cell numbers from each section were counted within the prelimibic and infralimbic cortex (see the scheme in the Fig. 2a). The number of cells of each subregion were averaged and normalised on area (mm^2). The challenge of co-localising proteins with different cellular positive cell detection, dependent on cell segmentation, remains unresolved in image analysis. We used state-of-the-art cell segmentation techniques, validated in a prior study published in Nature Communications[34], where the method's predictive validity was confirmed with functional experiments. While our approach reliably identifies $D1^+$ neurons, it may introduce minor systematic bias in D1 attribution, potentially underestimating $D1^+$ cells and overrepresenting $D1^-$ cells. However, this bias is unlikely to differ between groups injected with different SKF doses, ensuring a valid comparison of $c\text{-}Fos^+/D1^+$ neurons relative to total $c\text{-}Fos^+$ cells in each group.

Statistical analysis

Data were analysed with the Statview 5.0, Statistica 7, and GraphPad Prism 8 software. The significance level was set at $p < 0.05$ for all experiments. Data are expressed as mean ± standard errors (SEM). The

number of mice per group was calculated a priori with a power analysis using the G*Power 3.1 software with $\alpha = 0.05$, effect size = 0.6, and power $(1 - \beta) = 0.80$. Some of the animals were used for Western blot (PKA substrates) and histology. The exact sample size is reported in Supplementary Tables 9 and 10. Data were inspected for normal distribution through a Shapiro–Wilk test. One-way ANOVA was used to evaluate behavioural, biochemical, and immunohistochemical differences, followed with Tukey's post hoc analysis where appropriate. For single object comparisons, we used an ANOVA for repeated measures, with objects (six or eight levels) as repeated measures, followed by the Dunnett's post hoc analysis.

Reporting summary

Further information on research design is available in the Nature Portfolio Reporting Summary linked to this article.

Data availability

The data that support the findings of this study are available from the corresponding author upon request. The mass spectrometry phosphoproteomics data are available via ProteomeXchange with identifier PXD045107. Source data are provided with this paper.

References

1. Miller, G. A. The magical number seven, plus or minus two: Some limits on our capacity for processing information. *Psychol. Rev*. https://doi.org/10.1037/0033-295x.101.2.343 (1994).
2. Sannino, S. et al. Role of the dorsal hippocampus in object memory load. *Learn. Mem*. https://doi.org/10.1101/lm.025213.111 (2012).
3. Assecondi, S., Hu, R., Kroeker, J., Eskes, G. & Shapiro, K. Older adults with lower working memory capacity benefit from transcranial direct current stimulation when combined with working memory training: a preliminary study. *Front. Aging Neurosci*. **14**, 1–11 (2022).
4. Leonard, C. J. et al. Toward the neural mechanisms of reduced working memory capacity in schizophrenia. *Cereb. Cortex* https://doi.org/10.1093/cercor/bhs148 (2013).
5. Fuster, J. M. & Alexander, G. E. Neuron activity related to short-term memory. *Science* **173**, 652–654 (1971).
6. Brozoski, T. J., Brown, R. M., Rosvold, H. E. & Goldman, P. S. Cognitive deficit caused by regional depletion of dopamine in prefrontal cortex of rhesus monkey. *Science* https://doi.org/10.1126/science.112679 (1979).
7. Wilson, F. A. W., Scalaidhe, S. P. & Goldman-Rakic, P. S. Dissociation of object and spatial processing domains in primate prefrontal cortex. *Science* https://doi.org/10.1126/science.8316836 (1993).
8. De Leonibus, E., Verheij, M. M. M., Mele, A. & Cools, A. Distinct kinds of novelty processing differentially increase extracellular dopamine in different brain regions. *Eur. J. Neurosci*. https://doi.org/10.1111/j.1460-9568.2006.04658.x (2006).
9. Managò, F., Castellano, C., Oliverio, A., Mele, A. & De Leonibus, E. Role of dopamine receptors subtypes, D1-like and D2-like, within the nucleus accumbens subregions, core and shell, on memory consolidation in the one-trial inhibitory avoidance task. *Learn. Mem*. https://doi.org/10.1101/lm.1177509 (2009).
10. Attilio Iemolo, M. D. R. & Leonibus, and E. De. Role of dopamine in memory consolidation. *Nova Science Publishers, Inc*. **1**, 161-198 (2015).
11. Yang, Y. et al. D1 dopamine receptors intrinsic activity and functional selectivity affect working memory in prefrontal cortex. *Mol. Psychiatry* https://doi.org/10.1038/s41380-018-0312-1 (2021).
12. Zahrt, J., Taylor, J. R., Mathew, R. G. & Arnsten, A. F. T. Supranormal stimulation of D1 dopamine receptors in the rodent prefrontal cortex impairs spatial working memory performance. *J. Neurosci*. https://doi.org/10.1523/jneurosci.17-21-08528.1997 (1997).
13. Vijayraghavan, S., Wang, M., Birnbaum, S. G., Williams, G. V. & Arnsten, A. F. T. Inverted-U dopamine D1 receptor actions on prefrontal neurons engaged in working memory. *Nat. Neurosci*. https://doi.org/10.1038/nn1846 (2007).
14. Arnsten, A. F. T., Cai, J. X., Murphy, B. L. & Goldman-Rakic, P. S. Dopamine D1 receptor mechanisms in the cognitive performance of young adult and aged monkeys. *Psychopharmacology* https://doi.org/10.1007/BF02245056 (1994).
15. Cai, J. X. & Arnsten, A. F. T. Dose-dependent effects of the dopamine D1 receptor agonists A77636 or SKF81297 on spatial working memory in aged monkeys. *J. Pharmacol. Exp. Ther*. **283**, 183–189 (1997).
16. Arnsten, A. F. T. & Goldman-Rakic, P. S. Noise stress impairs prefrontal cortical cognitive function in monkeys: evidence for a hyperdopaminergic mechanism. *Arch. Gen. Psychiatry* https://doi.org/10.1001/archpsyc.55.4.362 (1998).
17. Williams, G. V. & Goldman-Rakic, P. S. Modulation of memory fields by dopamine D1 receptors in prefrontal cortex. *Nature* https://doi.org/10.1038/376572a0 (1995).
18. Runyan, J. D., Moore, A. N. & Dash, P. K. A role for prefrontal calcium-sensitive protein phosphatase and kinase activities in working memory. *Learn. Mem*. https://doi.org/10.1101/lm.89405 (2005).
19. Amico, F., Spowart-Manning, L., Anwyl, R. & Rowan, M. J. Performance- and task-dependent effects of the dopamine D1/D5 receptor agonist SKF 38393 on learning and memory in the rat. *Eur. J. Pharmacol*. https://doi.org/10.1016/j.ejphar.2007.08.039 (2007).
20. Granon, S. et al. Enhanced and impaired attentional performance after infusion of D1 dopaminergic receptor agents into rat prefrontal cortex. *J. Neurosci*. https://doi.org/10.1523/jneurosci.20-03-01208.2000 (2000).
21. Abi-Dargham, A. et al. Dopamine D1R receptor stimulation as a mechanistic pro-cognitive target for schizophrenia. *Schizophr. Bull*. **48**, 199–210 (2022).
22. Goldman-Rakic, P. S., Muly, E. C. & Williams, G. V. D1 receptors in prefrontal cells and circuits. *Brain Res. Rev*. https://doi.org/10.1016/S0165-0173(99)00045-4 (2000).
23. Dash, P. K., Moore, A. N., Kobori, N. & Runyan, J. D. Molecular activity underlying working memory. *Learn. Memory* https://doi.org/10.1101/lm.558707 (2007).
24. Gray, D. L. et al. Impaired β-arrestin recruitment and reduced desensitization by non-catechol agonists of the D1 dopamine receptor. *Nat. Commun*. **9**, 674 (2018).
25. Cimino, J. X., Zhou, M., Waxmonsky, J., Mailman, R. B. & Yang, Y. Characterization of behavioral changes in T-maze alternation from dopamine D1 agonists with different receptor coupling mechanisms. *Psychopharmacology* **240**, 2187–2199 (2023).
26. Yang, Y., Kocher, S. D., Lewis, M. M. & Mailman, R. B. Dose-dependent regulation on prefrontal neuronal working memory by dopamine D1 agonists: evidence of receptor functional selectivity-related mechanisms. *Front. Neurosci*. **16**, 1–17 (2022).
27. Sawaguchi, T. & Goldman-Rakic, P. S. D1 dopamine receptors in prefrontal cortex: involvement in working memory. *Science* https://doi.org/10.1126/science.1825731 (1991).
28. Roca, M. et al. The relationship between executive functions and fluid intelligence in schizophrenia. *Front. Behav. Neurosci*. **8**, 1–8 (2014).
29. Lud Cadet, J., Jayanthi, S., T. McCoy, M., Beauvais, G. & Sheng Cai, N. Dopamine D1 receptors, regulation of gene expression in the brain, and neurodegeneration. *CNS Neurol. Disord. Drug Targets* https://doi.org/10.2174/187152710793361496 (2012).
30. Cools, R., Gibbs, S. E., Miyakawa, A., Jagust, W. & D'Esposito, M. Working memory capacity predicts dopamine synthesis capacity in the human striatum. *J. Neurosci*. https://doi.org/10.1523/JNEUROSCI.4475-07.2008 (2008).

31. Olivito, L., De Risi, M., Russo, F. & De Leonibus, E. Effects of pharmacological inhibition of dopamine receptors on memory load capacity. *Behav. Brain Res*. https://doi.org/10.1016/j.bbr.2018.10.041 (2019).
32. Torromino, G. et al. Thalamo-hippocampal pathway regulates incidental memory capacity in mice. *Nat. Commun*. https://doi.org/10.1038/s41467-022-31781-8 (2022).
33. O'Sullivan, G. J., Roth, B. L., Kinsella, A. & Waddington, J. L. SK&F. 83822 distinguishes adenylyl cyclase from phospholipase C-coupled dopamine D1-like receptors: Behavioural topography. *Eur. J. Pharmacol*. https://doi.org/10.1016/j.ejphar.2004.01.004 (2004).
34. Soares-Cunha, C. et al. Activation of D2 dopamine receptor-expressing neurons in the nucleus accumbens increases motivation. *Nat. Commun*. **7**, 11829 (2016).
35. Lee, S. J. et al. Cell-type-specific asynchronous modulation of PKA by dopamine in learning. *Nature* **590**, 451–456 (2021).
36. Myeku, N. et al. Tau-driven 26S proteasome impairment and cognitive dysfunction can be prevented early in disease by activating cAMP-PKA signaling. *Nat. Med*. https://doi.org/10.1038/nm.4011 (2016).
37. Smith, F. D., Samelson, B. K. & Scott, J. D. Discovery of cellular substrates for protein kinase A using a peptide array screening protocol. *Biochem. J*. https://doi.org/10.1042/BJ20110720 (2011).
38. Olivito, L. et al. Phosphorylation of the AMPA receptor GluA1 subunit regulates memory load capacity. *Brain Struct. Funct*. https://doi.org/10.1007/s00429-014-0927-1 (2016).
39. Jones-Tabah, J., Mohammad, H., Paulus, E. G., Clarke, P. B. S. & Hébert, T. E. The signaling and pharmacology of the dopamine D1 Receptor. *Front. Cell. Neurosci*. https://doi.org/10.3389/fncel.2021.806618 (2022).
40. Nagai, T. et al. Phosphoproteomics of the dopamine pathway enables discovery of Rap1 activation as a reward signal in vivo. *Neuron* https://doi.org/10.1016/j.neuron.2015.12.019 (2016).
41. Dostmann, W. R. G. (RP)-cAMPS inhibits the cAMP-dependent protein kinase by blocking the cAMP-induced conformational transition. *FEBS Lett*. https://doi.org/10.1016/0014-5793(95)01201-O (1995).
42. Roth, B. L. DREADDs for Neuroscientists. *Neuron* https://doi.org/10.1016/j.neuron.2016.01.040 (2016).
43. Parthasarathy, H. B. & Graybiel, A. M. Cortically driven immediate-early gene expression reflects modular influence of sensorimotor cortex on identified striatal neurons in the squirrel monkey. *J. Neurosci*. https://doi.org/10.1523/jneurosci.17-07-02477.1997 (1997).
44. Paraskevopoulou, F., Herman, M. A. & Rosenmund, C. Glutamatergic innervation onto striatal neurons potentiates GABAergic synaptic output. *J. Neurosci*. https://doi.org/10.1523/JNEUROSCI.2630-18.2019 (2019).
45. Hippenmeyer, S. et al. A developmental switch in the response of DRG neurons to ETS transcription factor signaling. *PLoS Biol*. **3**, 0878–0890 (2005).
46. Montagne, G. Performance during learning. *J. Mot. Behav*. **39**, 491–502 (2007).
47. Kellendonk, C., Simpson, E. H. & Kandel, E. R. Modeling cognitive endophenotypes of schizophrenia in mice. *Trends Neurosci*. https://doi.org/10.1016/j.tins.2009.02.003 (2009).
48. Zhou, X. et al. Modulating NMDA receptors to treat MK-801-induced schizophrenic cognition deficit: effects of clozapine combining with PQQ treatment and possible mechanisms of action. *BMC Psychiatry* https://doi.org/10.1186/s12888-020-02509-z (2020).
49. Mandillo, S., Rinaldi, A., Oliverio, A. & Mele, A. Repeated administration of phencyclidine, amphetamine and MK-801 selectively impairs spatial learning in mice: a possible model of psychotomimetic drug-induced cognitive deficits. *Behav. Pharmacol*. https://doi.org/10.1097/00008877-200311000-00006 (2003).
50. Svoboda, J., Stankova, A., Entlerova, M. & Stuchlik, A. Acute administration of MK-801 in an animal model of psychosis in rats interferes with cognitively demanding forms of behavioral flexibility on a rotating arena. *Front. Behav. Neurosci*. https://doi.org/10.3389/fnbeh.2015.00075 (2015).
51. Vojtechova, I. et al. Dizocilpine (MK-801) impairs learning in the active place avoidance task but has no effect on the performance during task/context alternation. *Behav. Brain Res*. https://doi.org/10.1016/j.bbr.2016.03.020 (2016).
52. Yen, Y. C., Lung, F. W. & Chong, M. Y. Adverse effects of risperidone and haloperidol treatment in schizophrenia. *Prog. Neuro-Psychopharmacol. Biol. Psychiatry* https://doi.org/10.1016/j.pnpbp.2003.10.006 (2004).
53. Gilleen, J. et al. An experimental medicine study of the phosphodiesterase-4 inhibitor, roflumilast, on working memory-related brain activity and episodic memory in schizophrenia patients. *Psychopharmacology* **238**, 1279–1289 (2021).
54. Al-Amin, M. M. et al. Tadalafil enhances working memory, and reduces hippocampal oxidative stress in both young and aged mice. *Eur. J. Pharmacol*. **745**, 84–90 (2014).
55. Rosenbrock, H. et al. The novel phosphodiesterase 9A inhibitor BI 409306 increases cyclic guanosine monophosphate levels in the brain, promotes synaptic plasticity, and enhances memory function in rodents. *J. Pharmacol. Exp. Ther*. **371**, 633–641 (2019).
56. Tecuapetla, F., Matias, S., Dugue, G. P., Mainen, Z. F. & Costa, R. M. Balanced activity in basal ganglia projection pathways is critical for contraversive movements. *Nat. Commun*. **5**, 1–10 (2014).
57. Vicente, A. M., Galvão-Ferreira, P., Tecuapetla, F. & Costa, R. M. Direct and indirect dorsolateral striatum pathways reinforce different action strategies. *Curr. Biol*. **26**, R267–R269 (2016).
58. Bonnavion, P. et al. Striatal projection neurons coexpressing dopamine D1 and D2 receptors modulate the motor function of D1- and D2-SPNs. *Nat. Neurosci*. **27**, 1783–1793 (2024).
59. Hunger, L., Kumar, A. & Schmidt, R. Abundance compensates kinetics: similar effect of dopamine signals on D1 and D2 receptor populations. *J. Neurosci*. **40**, 2868–2881 (2020).
60. Okubo, Y. et al. Decreased prefrontal dopamine D1 receptors in schizophrenia revealed by PET. *Nature* https://doi.org/10.1038/385634a0 (1997).
61. Bubenikova-Valesova, V., Svoboda, J., Horacek, J. & Vales, K. The effect of a full agonist/antagonist of the D1 receptor on locomotor activity, sensorimotor gating and cognitive function in dizocilpine-treated rats. *Int. J. Neuropsychopharmacol*. https://doi.org/10.1017/S1461145708009851 (2009).
62. Horiguchi, M. et al. D1 receptor agonists reverse the subchronic phencyclidine (PCP)-induced novel object recognition (NOR) deficit in female rats. *Behav. Brain Res*. https://doi.org/10.1016/j.bbr.2012.09.030 (2013).
63. McLean, S. L., Idris, N. F., Woolley, M. L. & Neill, J. C. D1-like receptor activation improves PCP-induced cognitive deficits in animal models: Implications for mechanisms of improved cognitive function in schizophrenia. *Eur. Neuropsychopharmacol*. https://doi.org/10.1016/j.euroneuro.2009.01.009 (2009).
64. Duinen, M. et al. Treatment of cognitive impairment in schizophrenia: potential value of phosphodiesterase inhibitors in prefrontal dysfunction. *Curr. Pharm. Des*. https://doi.org/10.2174/138161282166615060511094l (2015).
65. Galizio, M. et al. Effects of NMDA antagonist dizocilpine (MK-801) are modulated by the number of distractor stimuli in the rodent odor span task of working memory. *Neurobiol. Learn. Mem*. https://doi.org/10.1016/j.nlm.2019.03.004 (2019).

66. Ceccarelli, F. et al. Static and dynamic coding in distinct cell types during associative learning in the prefrontal cortex. *Nat. Commun.* **14**, 8325 (2023).
67. Castro, L. R. V. et al. Striatal neurones have a specific ability to respond to phasic dopamine release. *J. Physiol.* https://doi.org/10.1113/jphysiol.2013.252197 (2013).
68. Reneaux, M. & Gupta, R. Prefronto-cortical dopamine D1 receptor sensitivity can critically influence working memory maintenance during delayed response tasks. *PLoS ONE* https://doi.org/10.1371/journal.pone.0198136 (2018).
69. Taylor, J. R., Birnbaum, S., Ubriani, R. & Arnsten, A. F. Activation of cAMP-dependent protein kinase A in prefrontal cortex impairs working memory performance. *J. Neurosci.* https://doi.org/10.1523/jneurosci.19-18-j0001.1999 (1999).
70. Tepper, J. M. & Bolam, J. P. Functional diversity and specificity of neostriatal interneurons. *Curr. Opin. Neurobiol.* **14**, 685–692 (2004).
71. Crump, F. T., Dillman, K. S. & Craig, A. M. cAMP-dependent protein kinase mediates activity-regulated synaptic targeting of NMDA receptors. *J. Neurosci.* **21**, 5079–5088 (2001).
72. Mallet, N., Le Moine, C., Charpier, S. & Gonon, F. Feedforward inhibition of projection neurons by fast-spiking GABA interneurons in the rat striatum in vivo. *J. Neurosci.* **25**, 3857–3869 (2005).
73. Massacci, G. et al. A key role of the WEE1-CDK1 axis in mediating TKI-therapy resistance in FLT3-ITD positive acute myeloid leukemia patients. *Leukemia* (2023) https://doi.org/10.1038/s41375-022-01785-w.
74. Michalski, A. et al. Mass spectrometry-based proteomics using Q exactive, a high-performance benchtop quadrupole orbitrap mass spectrometer. *Mol. Cell. Proteom.* https://doi.org/10.1074/mcp.M111.011015 (2011).
75. Ritchie, M. E. et al. Limma powers differential expression analyses for RNA-sequencing and microarray studies. *Nucleic Acids Res.* https://doi.org/10.1093/nar/gkv007 (2015).
76. Liao, Y., Wang, J., Jaehnig, E. J., Shi, Z. & Zhang, B. WebGestalt 2019: gene set analysis toolkit with revamped UIs and APIs. *Nucleic Acids Res.* https://doi.org/10.1093/nar/gkz401 (2019).
77. Reimand, J., Kull, M., Peterson, H., Hansen, J. & Vilo, J. G:Profiler-a web-based toolset for functional profiling of gene lists from large-scale experiments. *Nucleic Acids Res.* https://doi.org/10.1093/nar/gkm226 (2007).
78. De Leonibus, E., Oliverio, A. & Mele, A. A study on the role of the dorsal striatum and the nucleus accumbens in allocentric and egocentric spatial memory consolidation. *Learn. Mem.* https://doi.org/10.1101/lm.94805 (2005).
79. Paxinos, G. & Franklin, K. B. J. *The Mouse Brain in Stereotaxic Coordinates*, 2nd edition. (*Academic Press*, 2001).

Acknowledgements

We thank Dr. Cathal Wilson and Dr. Elizabeth Illingworth for critical and language revision of the manuscript; Dr. Graciana Diez-Roux for helpful suggestions; Prof. Fabrizio Gardoni and Prof. Alessandro Treves for helpful discussions, critical reading of the manuscript and for suggestions. We also thank Chiara Di Eugenio for drawing the graphical abstract with Biorender and Eng. Antonio Simonetti for his help in processing the counting data. This work was supported by grants from Biomarker (MUR/CNR) and National Recovery and Resilience Plan (NRRP), project "Cascata-MNESYS (PE0000006) - A Multiscale integrated approach to the study of the nervous system in health and disease" (DN. 1553 11.10.2022) to EDL and by the National Recovery and Resilience Plan (PNRR) project "SEE LIFE- StrEngthEning of Eurobioimaging to RDM. Part of the images used in the figure schematics were created with BioRender.com.

Author contributions

M.D.R. and E.D.L. conceived the study and most of the experiments. M.D.R. performed the behavioural experiments, the histology experiments, and data analysis, supported by A.I., F.G.A., and D.C. G.T., E.D.L., and D.C. and G.T. performed surgery and optogenetic experiments. D.C. performed experiments with PV-cre mice. A.C., R.D.M., and L.S. performed biochemical experiments, supervised by A.L., C.P.C., and M.C. X.B.C. helped to perform histology experiments and analysed phosphoproteomic data. F.S., C.C., and P.G. performed phosphoproteomic experiments. MDR drafted the original manuscript and together with E.D.L. and G.T. drafted the revised version. E.D.L. coordinated the study and wrote the final version of the manuscript with input from all co-authors.

Competing interests

The authors declare no competing interests.

Additional information

Supplementary information The online version contains supplementary material available at https://doi.org/10.1038/s41467-025-57788-5.

Correspondence and requests for materials should be addressed to Elvira De Leonibus.

Peer review information *Nature Communications* thanks the anonymous reviewers for their contribution to the peer review of this work. A peer review file is available.